Project Number: MQF-MQP 3145

Stirling Engine Design for Manufacture Using Recycled Materials Locally in Ghana

A Major Qualifying Project

Submitted to the Faculty of the

WORCESTER POLYTECHNIC INSTITUTE

in partial fulfillment of the requirements for the degree of

Bachelor of Science

by

Marika Bogdanovich
Mechanical Engineering

Julia Leshka Jankowski
Mechanical Engineering

Elizabeth DiRuzza
Mechanical Engineering

Sophie Kurdziel
Mechanical Engineering

MIRAD Laboratory and Design Development Lab

Submitted on March 24, 2022

Approved by:

Professor M. S. Fofana, PhD, Advisor

MIRAD Laboratory, Mechanical Engineering Department

Professor Robert Krueger, PhD, Co-Advisor

Dr. Hermine Vedogbeton, Co-Advisor

Design Development Lab, Department of Social Sciences and Policy

Abstract

Ghana citizens face unreliable and unaffordable electricity in their everyday lives that many in the western world take for granted. The team sought to find a cheap, sustainable, and reliable source of electricity for charging cell phones in remote places of Ghana. A Stirling engine is used to harvest the current-voltage supply required to charge cell phones in Ghana. In the Stirling engine assembly are a flywheel, piston-crank mechanism, pulley, belt, bearings, servomotor and a thermo-heat source flame. The performance of the Stirling engine is evaluated in terms of the possibility to replace the engine components with e-waste materials available in Ghana. Experimental testing, modeling, component design engineering and analysis were carried out to locate conditions for effectively generating the current-voltage supply for charging cell phones in Ghana. A current-voltage power supply of 4.8 and 5 volts were generated by the Stirling engine. An $R_aC_aL_a$ electric circuit for the servomotor in the Stirling engine assembly, which is analogous to the mechanical mass-dashpot-spring system was used to establish the necessary conditions for effectively producing the required voltage for charging cell phones in Ghana's remote places. The engineering design process, experimental work and analysis form the basis for the creation of guidelines for selecting and replacing the Stirling engine components with e-waste materials. The critical thinking and engineering work involved in producing the results of the MQP are the intellectual merits. Engaging with our Ghanian partners and the co-design activities highlight the broad impact of the MQP. The established performance conditions also guide the selection and replacement of the Stirling engine components with available e-waste materials in Ghana. We measured the amount of energy transfer as work to the components of the Stirling engine over some infinitesimal displacement in terms of the speed for producing the current-voltage supply into the charging system. A workable prototype of a Stirling engine that could be created using local materials was provided to the students and professors at Academic City University College (ACUC) in Ghana. The local materials include what is available at the e-waste site in Accra, Ghana. Using Ghana's local materials would provide WPI and ACUC students to extend the derived results in this MQP and to create a multitude of iterations of the new design.

TABLE OF CONTENTS

List of Figures

List of Tables

Acknowledgements

We would like to thank a few people who have supported us immensely through the past months. To start, our WPI advisors, Professor Robert Krueger, Professor Mustapha Fofana, and Dr. Hermine Vedogbeton, we thank them for all the guidance and time they have dedicated to us. As with many things in life our project saw lots of ups and downs but being able to reach out to the three of them and ask for help with anything made the process go much smoother.

We would also like to thank Barbara Furhman from the Mechanical Engineering department for assisting us in figuring out the financing of our project. Her help was crucial in its progression. Peter Hefti, also from the Mechanical Engineering department, specifically in Higgins Laboratories where we spent much of our time testing and working with the recycled parts. We thank him for providing the laboratory space and knowledge on how to use the equipment.

Lastly, to our partners in Ghana, Suali, Julian Bennett, Melinda Tatenda, Alice Abigail Tatenda Bere, and Farouk Tetty-Larbie. Working with all of them has been a pleasure. Suali, we thank him for sharing about his experience at the e-waste site and his knowledge on all that is related to the site. And lastly thanks to Julian for connecting us with all the others we worked with and for providing context for the importance of our project. It has been fantastic working with the team and for having this opportunity at WPI.

CHAPTER 1. STIRLING ENGINE AND ELECTRICITY ACCESS

1. Introduction

For the average person in Ghana or anywhere around the world, almost every aspect of life involves electricity in some form. Access to reliable, cheap electricity is something that is taken for granted by people who live in countries with 100% access to electricity. In 2016, 87% of the world's population had access to electricity (Ritchie & Roser, 2020), however, there are still disparities between countries. As of 2019 much of the world's countries have at least 90% access to electricity, as shown in Figure 1. Access to electricity as shown in this figure

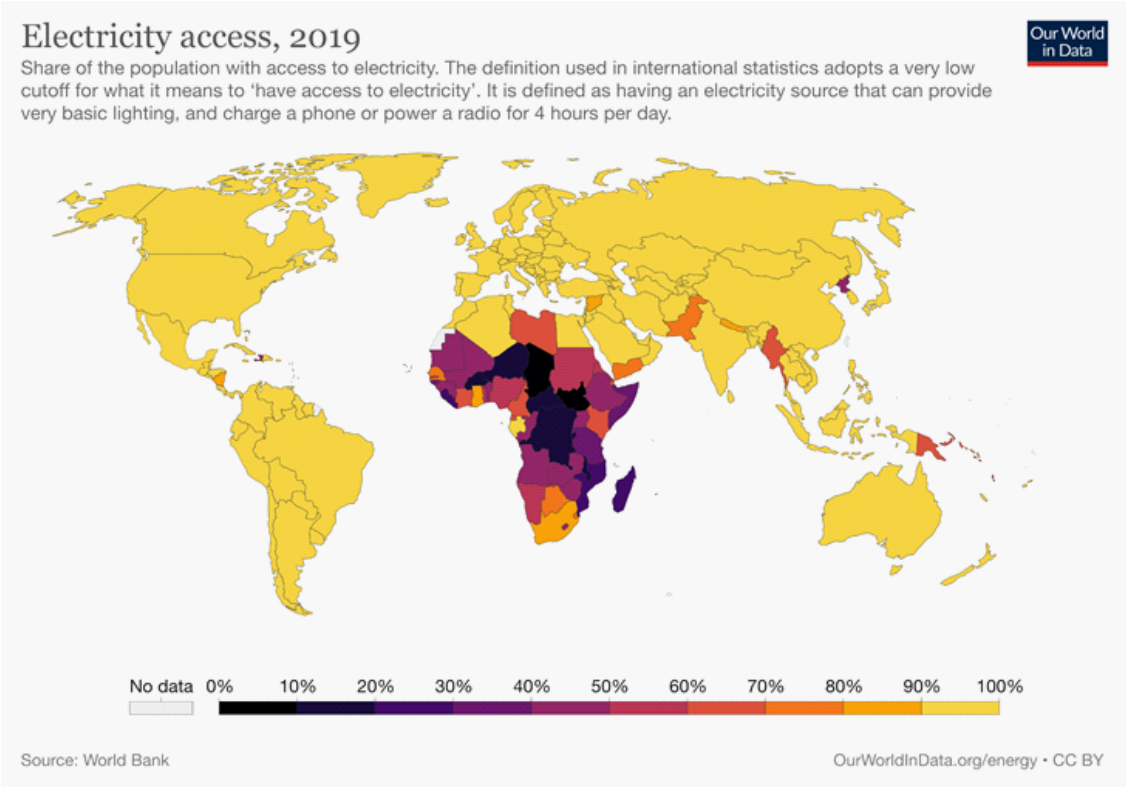

Figure 1: Map of electricity access around the world in 2019 (Ritchie & Roser, 2020)

is still a challenging problem in many parts of the world. In Africa a majority of the countries have electricity coverage of 60% or less. In some African countries, such as Chad, only 8.4% of the population has access to electricity as of 2019. This is a major issue that our project attempted to address. Ghana, a country in Africa, has a unique electricity situation since most of its citizens are on a grid system. Despite this, the

country experiences issues with reliability due to frequent blackouts. Sudden blackouts have been named "dumsors," by the Ghana residents and are a normal part of Ghanaian life with their daily occurrences (Owusu-Adjapong, 2018). Additionally, the cost of electricity is expensive compared to the average income of Ghanaian people. These electricity issues can create major problems for people who rely on electronic products, such as their cell phones. To help minimize this problem, we worked to co-design a Stirling engine out of electronic waste or e-waste that can locally be manufactured and repaired. In total, the cost of materials and labor needed to replicate this project would be lower in comparison to the price of electricity.

The project was intended to alleviate these issues while incorporating generative justice and co-design practices. The main goal of this project is to work towards a design of a Stirling engine using e-waste and recycled materials, for the purpose of charging a cell phone. This was accomplished through four objectives and they are:

• Investigate and reverse engineer a Stirling engine; this will help us better understand how the engine functions to help us later alter the material design.

• Develop a proof of concept; be able to better understand the basic function and purpose of the Stirling engine through the use of calculations and testing.

• Identify and evaluate e-waste materials; this will help understand which parts could have the potential to work on the Stirling engine.

• Component substitution; replace components in a functioning Stirling engine with materials collected from e-waste sites.

Within each objective, generative justice and co-design practices are implemented to ensure the partners in Ghana gain equally as much from the project as our team at Worcester Polytechnic Institute (WPI). Numerous tests were conducted in this project to better understand the workings of the Stirling engine. These tests were used to find fly-wheel speed, maximum voltage for charging cell phones, and engine efficiency. Additional tests were run on e-waste components to conclude if they were suitable replacements on the engine. Through data collection, the MQP team was able to shown that a Stirling engine can be used to charge a cell phone. A prototype servomotor was selected from an e-waste site and incorporated into the Stirling engine assembly. The Stirling engine

powered the servomotor, and the resulting voltage was used to charge a cell phone. We modeled the servomotor to evaluate performance and established performance regions for charging a cell phone efficiently. Major components of the Stirling engine were designed using standard engineering computer aided design tools. The testing of functions and performance of the Stirling engine powered servomotor and the charging of cell phone provided a better understanding of how the components in the engine assembly can be substituted with e-waste materials. Results from the testing and modeling guided the adjustments that can be made to maximize the voltage output for charging cell phones. Through research, experimental work and analysis we were able to create a prototype of the ideal Stirling engine, and provided the schematics to the team of students and professors in Accra, Ghana. Further research will be continued by the Academic City University College (ACUC) students to extend the MQP findings.

Stirling engines have been applied as energy sources since the 1870's when they were used for industrial projects in Great Britain. In the early 20th century, they fell out of favor and have almost been forgotten about over time. Stirling engines are simple designs and they run on any source of heat and can produce a small amount of electricity. Such engines could provide a great deal of opportunity for people across sub-Saharan Africa. The application of the Stirling engine to charge cell phones in remote places of Ghana could open other opportunities including the powering of a valve in a pump for an irrigation system, or running a ceiling or desk fan. The remaining parts of the report are described from Chapters 2 through the appendix sections. Chapter 2 reviews the background research and needed information for setting up the methodology. In this chapter applications of Stirling engine are also presented. Chapter 3 discusses the methods, experiments and analyses used to achieve the goals of the MQP and the processes involved. The modeling of the servomotor and performance regions for charging a cell phone efficiently are presented. Chapter 4 discusses the results from the data collection and calculations conducted. Guidelines for selecting and replacing e-waste materials with the components of the Stirling engine are presented. Chapter 5 is the conclusion where we summarize our findings and offer future recommendations for extending the work.

CHAPTER 2. STIRLING ENGINES AND THEIR APPLICATIONS

2. Introduction

Our team collaborated with the students and professors at Academic City University College in Ghana as well as people associated with the local e-waste management site in Accra to design and build a charging systems for cell phone use in Ghana. Based on the information we were provided through these conversations the team made informed decisions about what e-waste materials could be reused and recycled to replace parts of the Stirling engine prototype. Once these decisions were made the team worked with a local e-waste site in Massachusetts to receive e-waste materials similar to ones available in Ghana. Additionally, our contacts at Academic City have connected us with individuals who work at the e-waste sites to ensure we are properly utilizing the materials. The team then purchased an ideal Stirling engine to see how the engine functions without the use of recycled materials. The team provided the Ghana students with drawings of the ideal Stirling engine while they awaited the shipment of their own engine. The team conducted varying engineering tests on the engine, including the operation of the engine in three regions; overdamped, underdamped, and critically damped regions. From these tests the team was only able to charge a cell phone for a second due to resistance issues between the engine and the phone. The team concluded that the Stirling engine design needed more modifications than the team was able to make in our allotted time for the project before e-waste material substitutions can be applied. The Ghana student team took the results from our project and their access to their own ideal Stirling engine to continue their own tests and make the recommended modifications to the engine. Once the Stirling engines have been designed and tested, the drawings for the engine will be distributed to individuals at the e-waste site for them to produce and sell to Accra citizens for home use.

This Chapter describes the project and the relevant information researched to complete our methodology. The sections are as follows:

• Foundation of the Project; the circumstances that prompted the project and what we hope to accomplish.

• Ghana's electricity; the situation in Sub-Saharan Africa, specifically Ghana.

• E-Waste in Ghana; the e-waste available for use and how it relates to our project.

• History of the Stirling Engine; the invention as well as its prior uses.

• Stirling Engine Design; the common designs and the major components of the Stirling engine.

• Theoretical Stirling Engine Function; the process of the ideal Stirling cycle is described.

• Solar Power Stirling Engines; cases where solar energy has been used to power a Stirling engine.

• Required Component Materials; the important aspects to be considered when selecting materials for the components.

2.1 Foundation of the Project and Ghana's Energy Challenges

The major goal of this project is to design a Stirling engine for manufacture using locally available parts in Ghana that is capable of charging cell phones. This design would help the large majority of Ghana citizens who struggle with unreliable electricity sources. Although electricity in Ghana is widely available, it is unreliable due to chronic unpredictable power outages (Kumi, 2017). A combination of the Stirling engine design and the accessible Ghana e-waste site can provide the Ghanian citizens with reliable, sustainable energy. The Stirling engine was chosen as one possible solution because it is inexpensive and has a design that can be replicated using numerous component materials. A number of the required components can be replaced with parts from recycled appliances and electronics. This would repurpose these materials and could put them towards a sustainable and reusable application. E-waste sites have access to many second hand parts that can be repurposed to be used in a Stirling engine. Africa, including Accra, Ghana, has a large amount of e-waste materials imported from western locations. Due to Ghana's abundance of e-waste materials and their lack of reliable electricity, Stirling engines made of recycled e-waste materials could be a sustainable and accessible solution.

To make the Stirling engine an effective solution, we followed the criteria in Figure 2. The project criteria in this figure

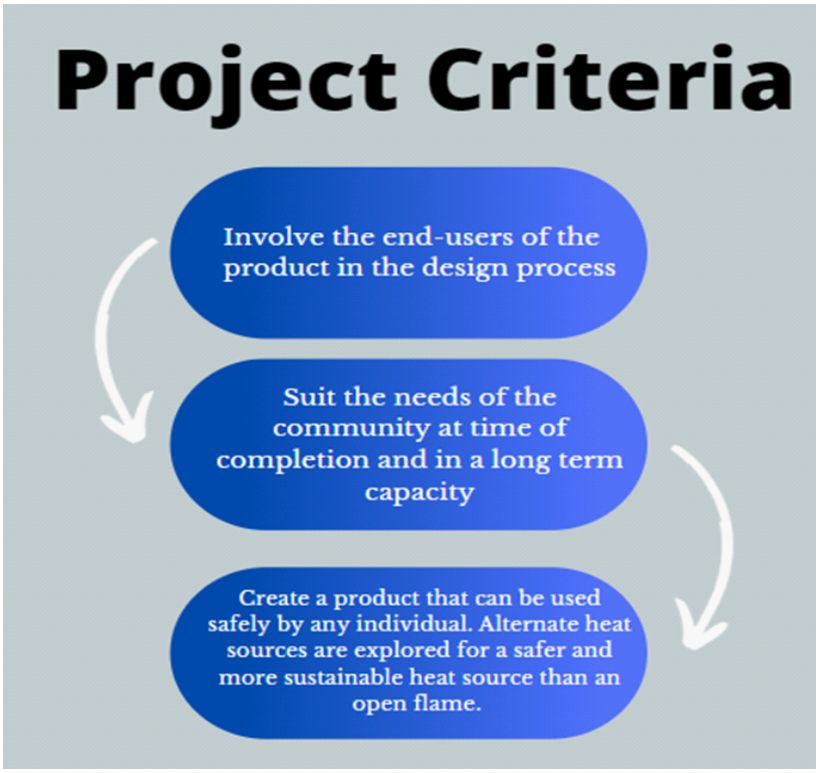

Figure 2: Established project criteria for realization

enable us to review a number of applications of Stirling engine. We also make use of the project criteria to select and use standard components for the Stirling engine design, servomotor and other components in the Stirling engine assembly. The project criteria ignited greater attention on the cost for manufacturing the Stirling engine, cell phone charging system and obtaining e-waste materials in Ghana.

2.1.1 Ghana's Electricity and Energy Harvesting Challenges

Ghana and its people continue to make effort to harvest electricity in a sustained way. The growth of new technologies, the collaboration with the developed world and drastic changes in the living standards influence Ghana's electricity harvesting greatly. Although there are particular lifestyles that continue with older methods of functioning, much of the world's population has shifted to using electricity for the majority of daily tasks. In wealthier, or countries that the United Nations defines as 'developed', electricity

is more widely used. This is due to easier access and a cultural dependence on it that has grown since electricity first became a part of the world. Accessibility and availability of electricity is a key component in the economic well-being of individuals and countries. In Sub-Saharan Africa, though, less than half the population has access to electricity as of 2018. Expanding accessibility is an important step to continued resiliency, however, this also comes at great cost. With the current rate of expansion in Sub-Saharan Africa, 60% of the population will have electricity access by 2030 (Valickova, 2021). These numbers are significantly different from electricity access rates across the globe. In fact, 95% of people who do not have access to electricity live in Sub-Saharan Africa, Latin America, and Asia (Panos, 2016). These regions face similar challenges in development, however, they also have the disadvantage of no electricity access. Although increasing access to electricity may be a slow and costly process, alternative individual-use electricity sources can be used as a supplement.

In regions where electricity is accessible, many communities continue to struggle with reliable electricity. Many issues arise from unreliable electricity supply such as slowdown in industrial activity, job and income losses, and disruptions in social life (Eshun, 2016). In regions of poor electricity reliability, the rate of development suffers the consequences of these power disruptions. There has been an increase in consumption and demand for electricity. This, along with limited investment in generation facilities, shortfalls in electricity imports, and institutional challenges have all played a part in Ghana's electricity supply shortages and unreliability (Nduhuura, 2021). Additionally, the cost of electricity in Ghana is a problem; compared to the average annual income, it is not affordable. Specifically in Accra, the average annual income is $883 with an average income range of $165 - $1100 (Akru, 2012). According to Enerdata, as of 2020, Ghana uses 485 kWh/capita of electricity per year. This amounts to an individual's yearly total of $77.60, based on electricity price data from SmartSolar Ghana. An individual making an average income uses 11% of their money on electricity. A study shows that households are able to pay only 8% of their incomes for electricity (Quartey, 2017). Therefore, the price of electricity is not affordable to the average Ghanaian population.

2.1.2 E-Waste in Ghana and Business Opportunities

E-Waste in Ghana and its reuse to make products create new business opportunities for many Ghanians. In Ghana, the growth in demand for consumer electronics has been tied to an increase in population and the general changing of consumer habits (Spitzbart, 2022). With an increase of electronics being purchased and used globally, there comes an increase in electronic waste. For many countries, the amount of waste they are producing is too much for them to manage independently. Such countries find other regions or countries around the world that are willing to take in their e-waste in return for various goods or services (Lepawsky et al., 2010). Through this, a massive e-waste site in Ghana has become internationally known for being the largest e-waste site on the planet (Daum et al., 2017). Old Fadama, pictured in Figure 3, is the digital waste dump in Accra, Ghana, but is more commonly known as Agbogbloshie. As seen in this figure

Figure 3: View of Agbogbloshie, Accra, Ghana (Kuma, 2011)

it is certain that the people and communities living near this e-waste site are impacted adversely in terms of their health and the environment by the toxic substances from some of the components of electronic waste or e-waste. As consumers, business and industries around the world focus on increasing their use of electronics, machines and devices, Ghana and other developing countries will continue to receive massive e-waste for recycling purpose, creating new business opportunities and bring to end of life circulation.

The area where the site is located in Agbogbloshie has grown into an informal settlement with a population of roughly 8,305 people as of the 2010 census (Cassels et al., 2014, p. 866). Many individuals depend on working at the site, with it being the sole place of residence for some. Everyday, the site collects trucks of e-waste from many countries around the world. It has become the job of the site workers to sift through and organize the component materials provided. The e-waste is then recycled and or resold within Ghana or exported to other countries. The site workers create business from the e-waste and make a living off of what other countries consider trash.

There are numerous risks involved with the work, disorganized system and environmental security challenges at Agbogbloshie. It is not uncommon to hear about unregulated e-waste disposal processes. In the United States for example, there are no national laws for managing e-waste; it is the responsibility of the state governments to implement and enforce regulations (Larmer, 2018). It is important to have regulations in place as the work involved in collecting and disposing of the electronic waste can be harmful to the environment and to those involved in the process. The informal economic activity in Ghana has become organized over time; associations, boards, and funding have all become implemented in the system. The Ghanaian Ministry of Environment, Science, Technology, and Innovation (MESTI) uses advisory services and international exchange to develop and effectively implement suitable e-waste regulations (Spitzbart, 2022). The Ghanaian government also recognizes a recently formed association of formal recycling enterprises to further this. The site in Agbogbloshie still struggles with environmental and health issues, however, so much economic empowerment and dependency lies at the hands of the workers who would not be able to make a living without the site (Grant et al., 2013). This abundance of e-waste present in Ghana provides an excellent source of materials that can be repurposed. This combined with the inconsistency in access to electricity are two parts of the foundation of our project. The remaining aspect is the Stirling engine which will be explained in the following sections starting with its history.

2.2 History and Applications of Stirling Engine

The Stirling engine was originally invented to compete with the steam engine in the early 1800s. Stirling engines are quiet, non-polluting, and a reliable method to generate power. These engines use external heat sources to vary the temperature of a gas (Church et al., n.d.). Robert Stirling, known as the father of the Stirling engine, filed for the Stirling engine patent in 1816 in Edinburgh, Scotland. The patent application was titled Improvements for Diminishing the Consumption of Fuel and in particular an Engine capable of being Applied to the Moving (of) Machinery on a Principle Entirely New (Brahambhatt, 2021). Included in the patent was an explanation of the construction and use of a regenerator as well as the first-ever description of a closed-cycle hot air engine system (Brahambhatt, 2021). What is known as a regenerator today, was an economizer or heat exchanger that Stirling used in his design (Church et al., n.d.). Figure 4 depicts a portrait of Robert Stirlingwho wanted to create a device to replace the steam engine as

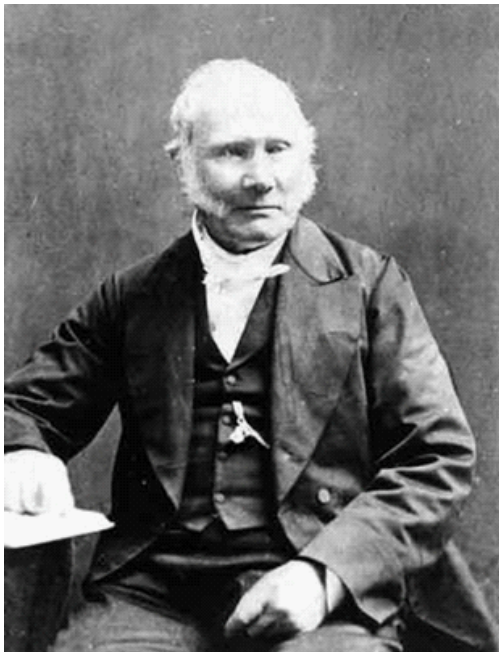

Figure 4: Robert Stirling (Linda Hall Library, 2019)

these engines would often explode and could cause many injuries to workers (Church et al., n.d.). Robert Stirling's engine design would be a safer alternative since it functions at lower pressures and stops if the heater section fails (Church et al., n.d.). Another

notable benefit is that the engine runs on external combustion, which can be designed to perform with high efficiency and therefore contribute little to no air pollution (Walker, 1973). Figure 5 shows a model of the Stirling engine from which it can be seen that

Figure 5: Model of Stirling engine at the National Museum of Scotland (Linda Hall Library, 2019)

the components then are much heavier than the components used in modern Stirling engine applications. James Stirling, Robert Stirling's brother and partner, presented at the Institution of Civil Engineers in 1845 and emphasized that the Stirling engine was not only aimed at saving fuel but also could serve as a safer alternative to the steam engine. In the steam engines widely used, the boilers would often explode, causing numerous injuries and deaths. Although this is not possible with the use of Stirling engines, they do not perform well at higher temperatures and fell out of commercial use due to frequent cylinder failures (Brahambhatt, 2021). Another issue of the Stirling engine is the comparative size; to see similar results as a steam engine, the Stirling engine would need to be significantly larger. The cost of the production and size barriers was what eventually led to the Stirling engine becoming less successful. As a consequence of their lack of presence at the commercial level, Stirling engines were overlooked for

many years. In 1938, the Philips company took interest in the design and licensed numerous patents. By 1952, Philips had developed a power generator with the Stirling engine system as a drive. This never went into mass production, but the research work conducted by Philips later led to development of cryogenic cooling systems and other successes (Brahambhatt, 2021). In recent years, Stirling engines have been used for submarines where they are able to extend the period spent underwater from a few days to weeks. The use of Stirling engines also allows for the submarine to be much quieter during travel; a large advantage for situations where concealment is necessary (nms.ac.uk, n.d.). In every design of a Stirling engine there are a number of components that are essential to its function. These components as well as the necessary conditions are discussed in the following section.

2.2.1 Stirling Engine Components Design and Manufacture

Stirling engines use heat as a way to produce power. Stirling engines are a type of external combustion engine. The average Stirling engine has seven main components: the piston, cylinder, flywheel, connecting rod, crankshaft, gas, and external heat source. These components can be arranged to form the three main types of Stirling engines: the alpha engine, the beta engine, and the gamma engine (Denno, n.d.). The first Stirling engine type is the alpha Stirling engine design which incorporates a configuration of two pistons in two different cylinders. One cylinder is connected to a cooler and the other to a heater, with the heated cylinder involved with expansion and the cooler side involved with compression as shown in Figure 6.

As seen this figurethe cylinders are connected together with a regenerator shaft. This

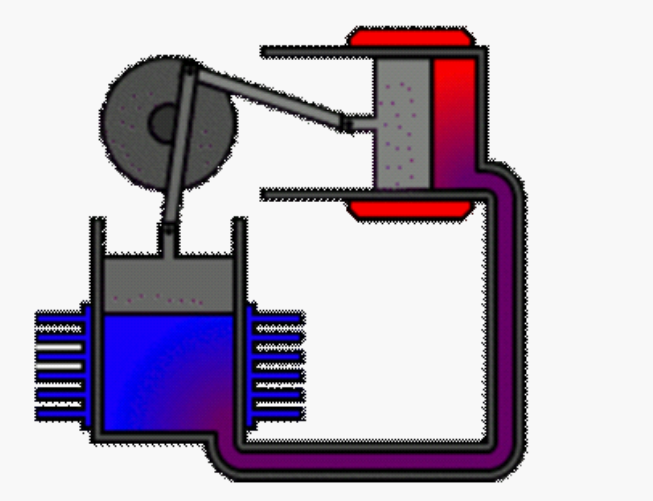

Figure 6: Alpha Stirling engine design (Urieli, 2013)

configuration is the simplest design of a Stirling engine and the separation of the two cylinders prevents premature mixing of the hot and cold fluids (Chen et al., 2014). The second Stirling engine type is the beta Stirling engine design which includes a singular cylinder, a power piston, and a displacer piston. The displacer piston moves the air between the cold and hot cylinders of the engine. This causes a change in the pressure between the cylinders which moves the piston back and forth as shown in the figure

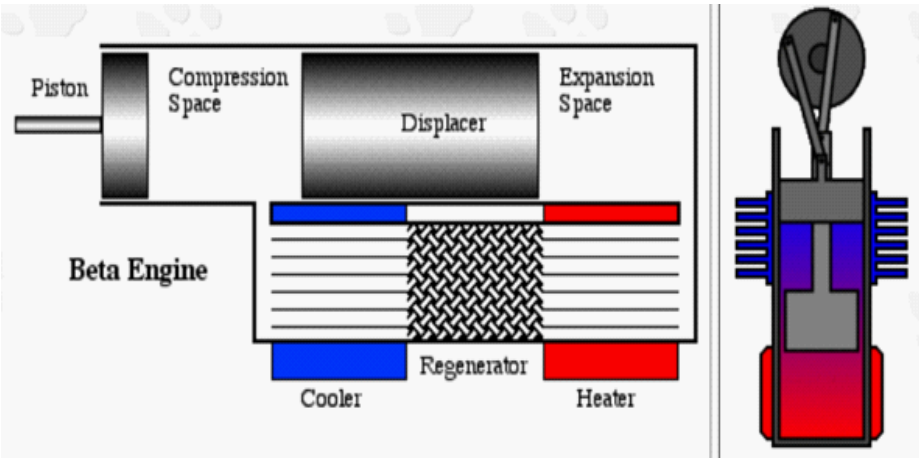

Figure 7: Beta Stirling engine design (Urieli, 2013)

In this Stirling engine as shown in Figure 7, the power piston and displacer move such

that the gas compresses while passing over the cooler section of the engine and expands while it passes over the heater area as shown in Figure 7 (Urieli, 2013). The last Stirling engine type is the gamma Stirling engine design which has a power piston and a displacer, but unlike the beta design, the power piston and the displacer are in different cylinders as seen in Figure 8. In this figure

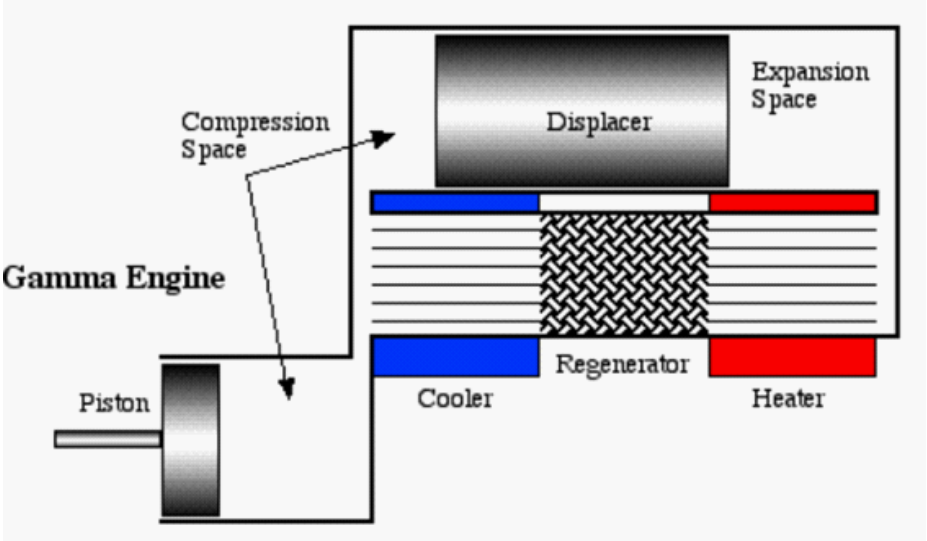

Figure 8: Gamma Stirling engine design (Urieli, 2013)

the cylinder that has the displacer piston also has the cooler and heater attached to it (Urieli, 2013). One side of the cylinder is heated and the other side of the displacer is cooled by the cooling fins. The downside to this design is that some of the expansion process has to occur in the compression space, leading to reduced output of specific power (Urieli, 2013). Although there are different mechanical designs of the Stirling engine, material properties for each have the same requirements. For example, the cylinders must be able to tolerate the temperatures of the heat source without deformation as well as maintaining the temperature difference between the hot and cold cylinder. The materials used in the Stirling engine are chosen to allow the engine to have its peak performance.

2.2.2 Component Materials and Their Selection

The Stirling engine block is typically made of cast ductile iron or aluminum alloy. For low temperature differential (LTD) Stirling engines, the internal components of the engine tend to be made of cast ductile iron or aluminum alloy, however, this can change depending on the required strength or heat resistance. As stated previously, the seven main components of a Stirling engine are the piston, cylinder, flywheel, connecting rod, crankshaft, gas, and external heat source. The piston and connecting rod are typically made of aluminum alloy due to its lightweight (Çinar et al., 2012). The power cylinders are made of brass. Another component, known as the displacer piston, can have different material that depends on the temperature differential. For example, in 1992 a Stirling engine was built that had a temperature difference of 1.8°C and the displacer was made of Styrofoam^{TM}. In the same engine, the piston was made of graphite (Çinar et al., 2012). In a more recent experiment, medium density fiberboard (MDF) was the highest performing material for a LTD Stirling engine as it provided more power compared to an aluminum alloy displacer (Çinar et al., 2012). The application of the engine will determine the temperature differential and thus the material needed on the engine. The temperature differential is caused by the heating and cooling of the cylinders, this process is known as a thermodynamic cycle and is explained in the following sections.

2.2.3 Theoretical Stirling Engine Functions and Cycles

With the heating and cooling of the cylinders, the piston moves and causes the flywheel to rotate. Although all engines are designed to move a piston, Stirling engines are unique due to functioning using a closed system of working fluid (Nice, 2021). Since the working fluid is in a closed system, the Stirling engine can function on an external heat source. This process is known as the Stirling cycle and is one of many thermodynamic cycles. There are a number of thermodynamic cycles that are used to transform heat energy into mechanical energy. In such heat engines, the working fluid, typically a gas, is heated which causes the expansion that moves the piston. The major properties of thermodynamic cycles are pressure, temperature, volume, and the working fluid. From these, the work done by the engine and the efficiency of the engine can be determined. The thermodynamic cycle that is the most efficient is the Carnot cycle (Lutz et al.,

2002). This is a theoretical cycle that has been designed for the steps in the process to be adiabatic and reversible; meaning throughout the cycle there is no heat or mass lost to the surroundings. Although the Carnot cycle is the most efficient, it is idealized and therefore not fully representable in a functioning engine. Although this is true of all heat cycles and engines, the Stirling cycle approaches the theoretical efficiency of the Carnot cycle and is appealing due to the ability to utilize waste heat.

The Stirling cycle consists of two ideally isochoric (constant volume) steps and two ideally isothermal (constant temperature) steps (Dimian et al., 2014). The pressure-volume (P-V) and temperature-entropy (T-s) diagram of the cycle is shown in Figure 9. In these figuresthe four properties correspond to the mechanical function of the engine.

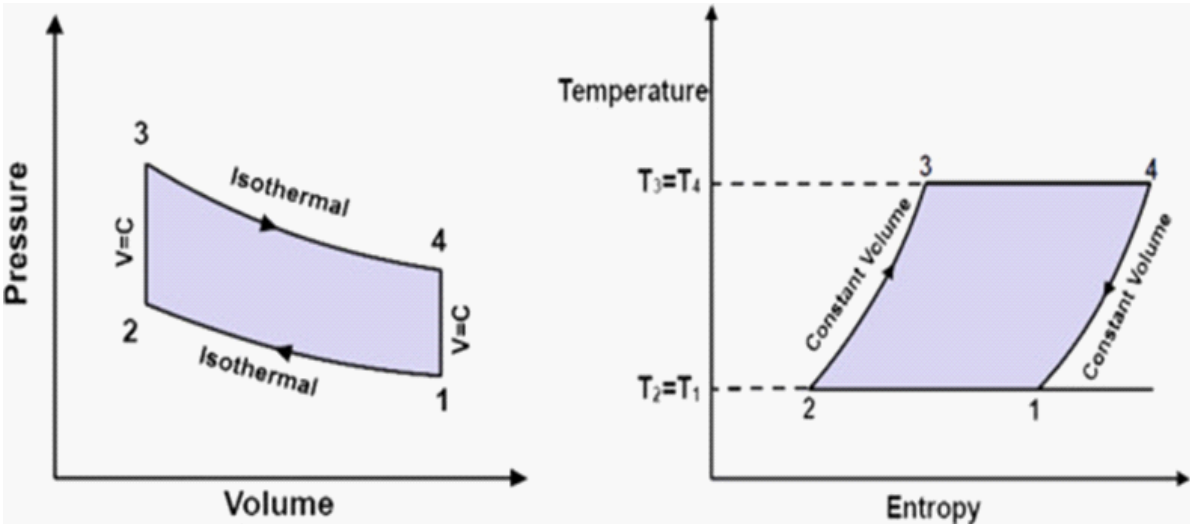

Figure 9: P-V and T-s diagrams of the Stirling cycle (Zohuri, 2018).

With every change in volume coinciding with the movement of the piston. The movement of the piston as it relates to the Stirling cycle is shown in Figure 10.

The diagrams in Figure 10

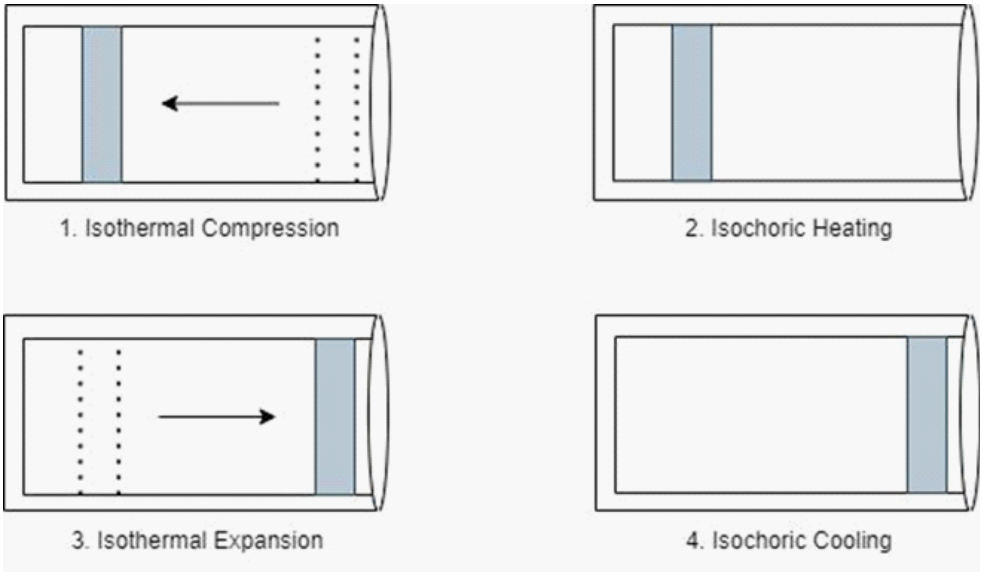

Figure 10: Location of the piston in the cylinder.

show the thermodynamic characteristics of the Stirling engine when it is subjected to an external heat source. These characteristics are described as follows:

1. In the first step of the cycle, the working fluid undergoes isothermal compression. During this step the pressure increases as the volume decreases and correlates to the piston moving towards the closed end of the cylinder.

2. The second step is isochoric meaning the working fluid is then kept at a constant volume as the pressure and the temperature are increased.

3. The third step is the system's second isothermal process, now with the working fluid undergoing a decrease in pressure and an increase in volume. As the gas expands, it applies pressure to the piston which is then pushed to the end of the cylinder.

4. The last step in the cycle is again isochoric as the working fluid cools. The sliding movement of the piston can then be used to turn a flywheel and furthermore to generate a charge.

These four steps occur rapidly, providing the flywheel with thousands of revolutions per minute. Although the most commonly used fuel in engines is a liquid combustible, Stirling engines require only a temperature difference; heat sources such as steam or the sun can be utilized by a Stirling engine (Kongtragool et al., 2003).

Solar energy is not only sustainable but also one of the most cost-effective sources of heat. Using solar energy to power a Stirling engine would provide a cheap and sustainable source of power. The use of solar powered Stirling engines has existed since 1864, when John Ericsson invented a solar powered hot air engine that utilized a reflector to heat the hot cylinder end of the displacer (Kongtragool et al., 2003). Creating a focused point of solar energy onto the hot cylinder of an alpha design type Stirling engine provides the needed heat source for the engine to produce power. In this process solar power is converted into mechanical energy, which can then further be converted into electrical power, thus using the solar energy to create an electrical output. Solar collectors are a special kind of heat exchanger, but the concave design has to incorporate a way to trace the sun due to its angle. However, flat-plate collectors do not need to trace the sun and could be a possible application for the purposes of our project (Tavakolpour et al., 2008). Apart from being sustainable, the use of solar power for the Stirling engine design allows for a safer heat source that is more easily controlled than that of fire.

CHAPTER 3. STIRLING ENGINE AND CELL PHONE CHARGER

3. Introduction

The following section introduces the methods employed to achieve the goal of our project and the materials involved in those processes. We begin by discussing the objectives set by the team that aided in fulfilling the project goal. From there, we elaborate on our collaboration with the Academic City University College (ACUC) students and their contributions to this project. We then evaluate our ethical responsibilities and how they were addressed throughout the project work and report writing. With the project goal to design a Stirling engine utilizing e-waste components, we set objectives to guide the course of the project work:

- Stirling engine investigation and reverse engineer
- Proof of concept
- Identifying e-waste materials
- Component substitution

Before any redesigning could take place, initial Stirling engine research was done to form an understanding of the function and intent of the components in the Stirling engine. After reverse engineering an 'ideal' Stirling engine, the team conducted tests and calculations to ensure charging a phone was possible. Then, the available e-waste materials were investigated and assessed with respect to the project. Various components of the Stirling engine were reviewed for the replacement and substitution with recycled materials. Throughout these objectives there was open communication with the student team at ACUC to effectively utilize the co-design process.

3.1 Stirling Engine Investigation and Reverse Engineering

Gaining a complete understanding of the function and components of Stirling engines is necessary to be able to make e-waste substitutions. To accomplish this, a Stirling engine kit was purchased, as shown in Figure 11. The team assembled the Stirling engine as seen in the figure

and this purchased Stirling engine kit from Amazon.com provided an opportunity for our team to gain a physical understanding of the alpha Stirling engine design while also allowing for more time to be spent on the proof of concept and material substitution

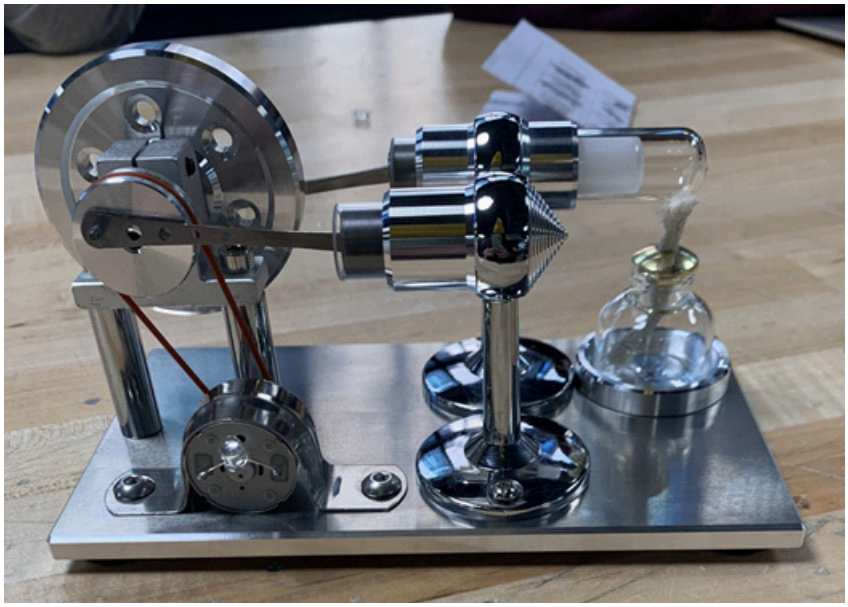

Figure 11: Assembled Stirling engine kit (original engine)

portions of the project. The alpha design of the engine was chosen due to the background research the team conducted. It was decided that the alpha design was the simplest of the Stirling engine designs. This engine will be referred to as the original engine. The original engine was considered the 'ideal' Stirling engine, meaning it was manufactured and did not include any replacement e-waste parts. It was chosen due to its size and advertised voltage output. This Stirling engine was stated to have a voltage output range of five to nine volts, aligning well with the five volt minimum needed to charge a cell phone.

After the original engine was received the first step was to observe how it performed. This was done by first finding a fuel source, in this case it was 90% isopropyl alcohol. The fuel was put in the glass jar that was provided and the wick was soaked in the fuel. The wick was then placed under the hot cylinder and lit and after waiting an appropriate time for the cylinder to heat up the flywheel was manually spun for the engine to start. A voltmeter was used to test the output voltage from the motor. After observing the Stirling engine's function, it was disassembled to be reverse engineered. All components' critical dimensions were measured using calipers and recorded on preliminary hand drawings. Using the computer aided design program SolidWorks, we modeled the Stirling engine.

This allowed us to communicate more effectively with the student team at ACUC in Ghana and perform finite element analysis on each component as well as the full assembly. Shown in Figure 12 is the finished assembly; further SolidWorks models and drawings can be found in Appendix A. The CAD model seeing in this figure and those extended models

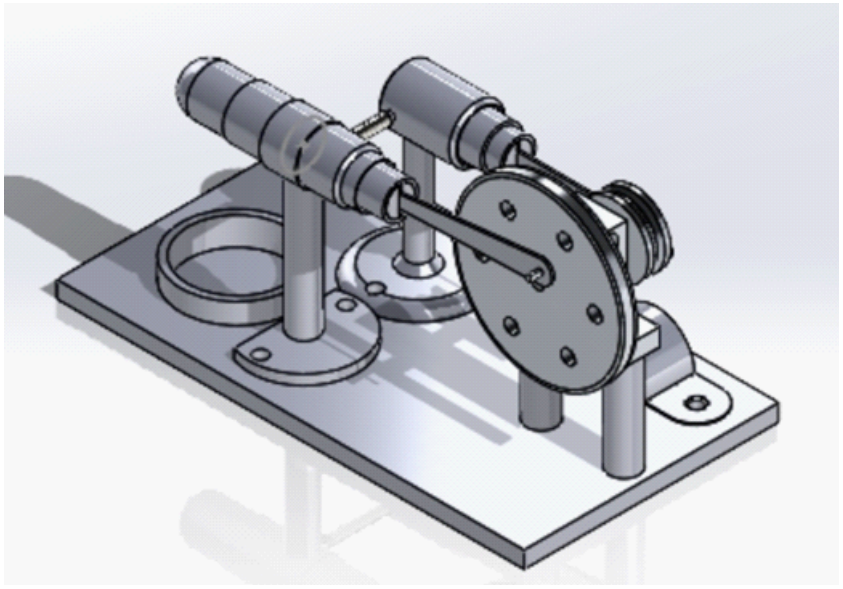

Figure 12: SolidWorks assembly of the Stirling engine kit

of the Stirling engine in Appendix A were created using WPI Engineering computer tools. Modifications were made to the original Stirling engine to ensure it is able to reach five volts, this is further covered in the results section. After the disassembly process of the original Stirling engine, the team purchased a second engine, hereafter referred to as the new engine, from Enginediy.com for additional testing. We utilized the same tests for the new engine that were applied to the original engine. The new engine is pictured in Figure 13.

This Stirling engine in this figure

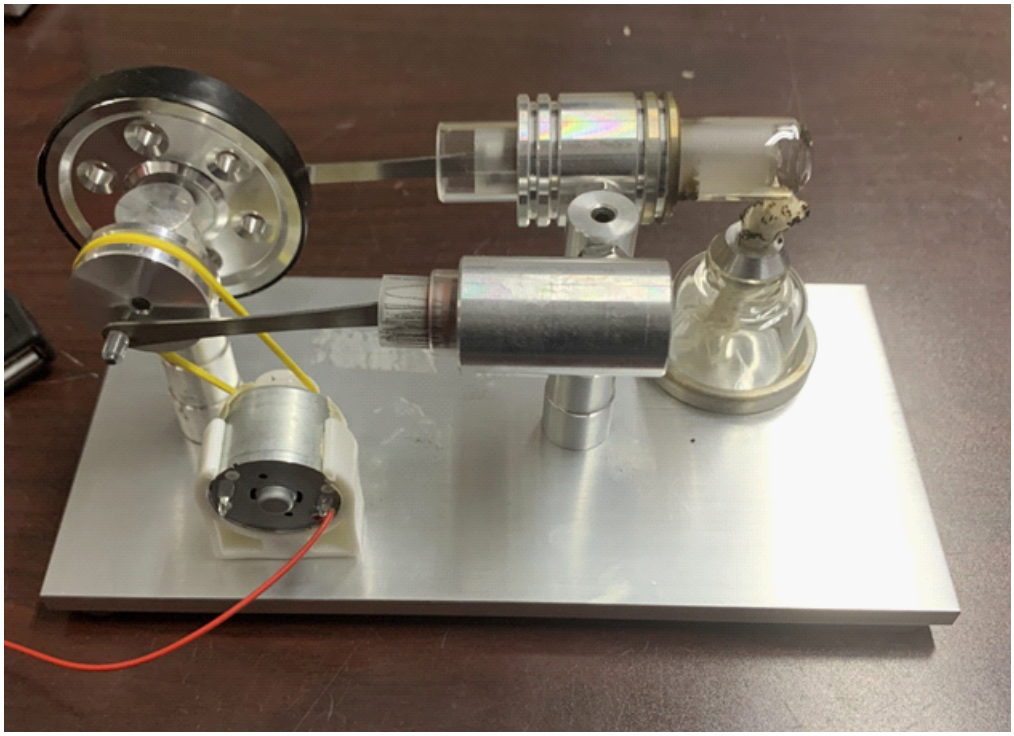

Figure 13: New Stirling engine kit purchased (second engine)

was used in the experiment to verify the production of the required voltage by the Stirling engine for charging cell phones The data collected through testing was used in the component substitution process to ensure the properties of the new materials were comparable to the replaced components.

3.1.1 Proof of Concept and Co-Design Activities

Proof of concept meant running tests and calculating if the ideal Stirling engine we purchased could in fact charge a cell phone like our goal hoped to achieve. These tests included measuring the surrounding air temperature and running the engine to see if it had higher performance in colder or warmer temperatures. We conducted tests to see how long it would take for the engine to get to maximum voltage, and then after extinguishing the flame, how long it took for the voltage to reach zero volts. Lastly, we performed a number of tests to experimentally determine the angular velocity of the flywheel. This furthers our understanding of the relation between the thermodynamic cycle and the function of the ideal Stirling engine.

To test the efficiency of the Stirling engine in varying temperatures the team used a thermometer to test the air temperature while running the engine. These tests were run in varying environments including a heat controlled room and the outside temperature on days of varying weather. When testing how long it took the engine to reach its maximum output voltage the team started by using a stopwatch application on our mobile devices and clicked start once the fire was lit underneath the hot cylinder. We then proceeded to spin the flywheel every five seconds to test how long it took for the hot cylinder to heat up enough for the engine to start moving on its own. Once the engine began to move autonomously a lap was added on the stopwatch. The team then observed the voltage output until it reached a consistent maximum voltage. The stopwatch was then lapped again and the time that it took to reach its maximum was recorded. The fire was then extinguished and the stopwatch continued timing until the voltage output was zero and the flywheels were stationary. All results were recorded.

The last test that we conducted was a flywheel speed test. The team conducted the flywheel speed test at the same time as the time tests for they are independent from one another. The speed test was done by using a tachometer device. The tachometer works by tracking a reflective piece of tape as it produces a laser aimed at the target of the readings. Due to the flywheel itself being reflective the team used black electrical tape to cover the side of the flywheel that was to be measured to ensure that the reflective material would not disrupt the readings.

The team then put a piece of the reflective tape over the electrical tape and started the engine as seen in Figure 14. This figureshows another view of the Stirling engine

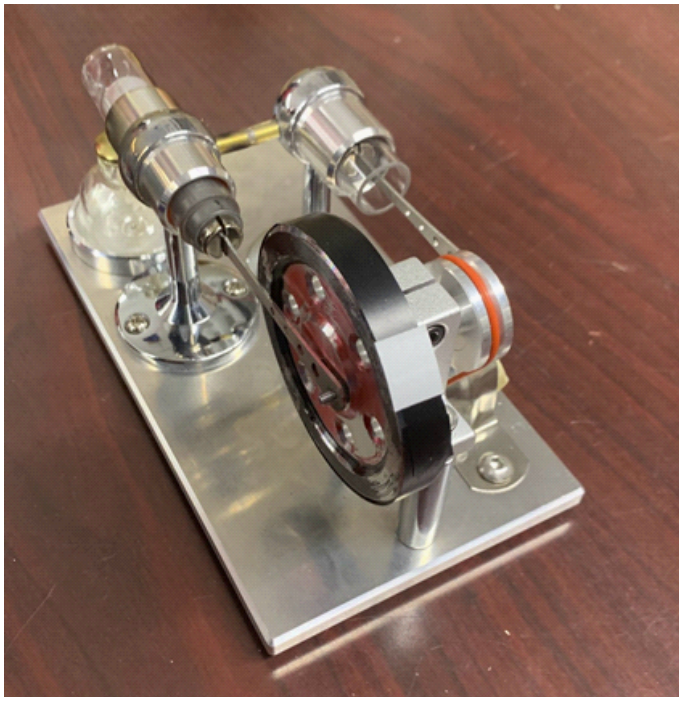

Figure 14: The Stirling engine prepared for flywheel speed testing

that was used in the laboratory for testing. The measurements were taken once the engine reached its maximum output voltage by aiming the tachometer over the flywheel where the reflective tape was attached. All results were recorded. The Stirling cycle is a thermodynamic process that is used on Stirling engines and other Stirling devices.

Figure 15 shows these cycles and in this figure

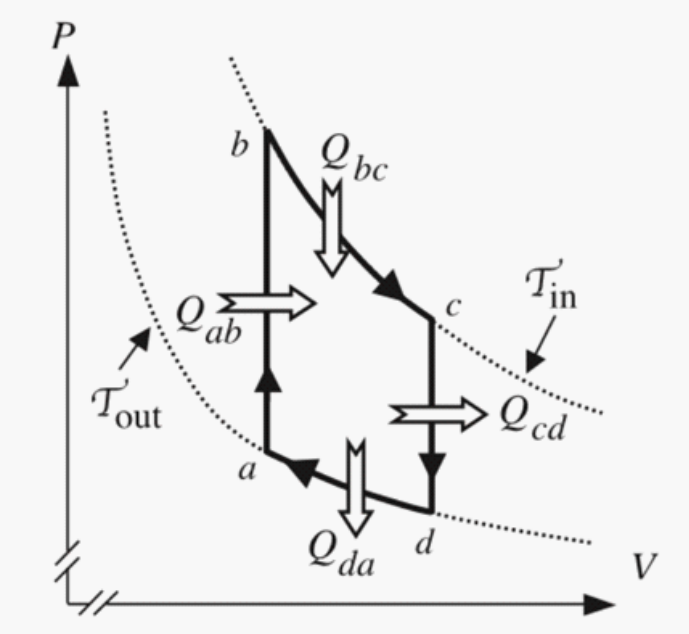

Figure 15: The Stirling Cycle PV Diagram

the parameter p is the pressure and v is the volume. This figure is referred to as pressure-volume or $p - v$ diagram for the Stirling Cycle. As previously stated, this cycle contains isochoric and isothermal processes. In an isochoric process the volume stays constant and the temperature and pressure change. In an isothermal process the temperature stays constant and the volume and pressure change. During the isochoric process, since the change in volume is zero there is no work done W given by the equation

$$W = \int_{v_i}^{v_f} p dv, \tag{1}$$

where p is the pressure, v_i is the initial volume and v_f the final volume. From the gas equation $pv = nRT$, we express the volume v a subject of the formula and substitute the

result into the work done equation (1) lead to

$$\begin{aligned} W &= \int_{v_i}^{v_f} p dv \\ &= nRT \int_{v_i}^{v_f} \frac{1}{v} dv \\ &= nRT(\ln v_f - \ln v_i) + \ln C \\ &= nRT \ln(C\frac{v_f}{v_i}). \end{aligned} \tag{2}$$

In this equation, $\ln C$ is the constant of integration, n is the amount of working fluid in moles, R is the ideal gas constant, and T is the temperature. Given the work formula in the equations (2), it can be assumed that all of the work done in the Stirling cycle is done during the isothermal process. Solving for the constant of integration for zero boundary condition yields the equation for the mechanical work

$$W = nRT \ln(\frac{v_f}{v_i}). \tag{3}$$

Within the natural log is the compression ratio, the ratio of the maximum volume of the engine to the minimum. This simplifies the calculation of the engine thermal efficiency η, which is given by the equation $\eta = \frac{W}{Q}$ where Q is equal to the heat input to the engine to allow for continuous cycling. The SI unit for work, energy and heat is joule which kilogram-meter squared per second squared or Newton-meter. The power p that the engine produces can be found using the equation $p = \omega\tau$ where the parameter ω is the angular speed of the engine's flywheel and τ is the torque. The magnitude of the torque τ can be found by multiplying the tangential force F of the spinning flywheel by the perpendicular distance d to the force. The SI unit for power is the Newton-meter per second, which is watt, and it is named after James Watt who spent enormous effort to improve the performance of steam engines. In the horsepower is commonly used as a unit for power and one horsepower is equivalent in the USC system of units as 3.3×10^4 $ft.lb/\min$ or 5.50×10^2 $\frac{ft.lb}{\sec}$. The heat input Q into the Stirling engine is the sum of all the heat quantities greater than zero. This can be found using the equation $Q = mc\Delta T$ where m is the mass of the working fluid, in this case air, c is the isovolumetric heat

capacity of air, and ΔT is the change in temperature of the Stirling engine system. Since the full output of the heat source will not be evenly received by the Stirling engine, this equation is used to approximate the total heat input.

Generally physical quantities may be measured in both the *International System (SI) and US Customary (USC) or British systems* of units. Changing from the SI to USC system of units is achieved by the conversion formula $SI/USC = \gamma$ where γ is the conversion factor. An inch is 2.54 centimeters, $1ft = 0.348m$ and 1 $kilometer = 0.592$ $mile$. The conversion of feet to inches is 12 $in = 1ft$, meter to kilometer is 1000 $m = 1$ km and hour to seconds is $1hr = 3600$ seconds. The ratio $SI/USC = \gamma$ is unique since it has the same dimensions in the SI and UCS systems of units. A dimension is the basic measure of a physical quantity and it has a number with a unit. One meter of length in the SI system equals to 3.281 feet in the USC unit system and 39.37 inches is one meter. A kilogram is the SI unit for mass and it is expressed in the USC unit system as slug using the conversation ratio $slug/kg = 14.59$. A slug is $lb.\sec^2/ft$ and one slug is 1.46×10^4 grams. The USC unit of weight is pound when the gravitational acceleration $g = 32.2ft/\sec^2$ and mass in slug. Consistency of units in equations and constitutive relations is essential for obtaining rational answers to a problem. It is suggested to always verify the units of quantities in the equations and constitutive relations before numerical values are substituted for the parameters.

3.1.2 Identifying and Evaluating E-Waste Materials

Before the Stirling engine components can be substituted with e-waste, an understanding of the materials available had to be achieved. To accomplish this, we visited a local e-waste site, spoke with an e-waste worker in Ghana, and gathered materials for assessment. The visit to the Wachusett Watershed Regional Recycling Center in West Boylston, Massachusetts provided us with first-hand knowledge of the available materials and their condition. We assumed that the e-waste available to us locally is similar to what is locally available to our partners in Ghana. To confirm this assumption, we asked Julian Bennett, the advisor to our team from ACUC, to help us get in contact with an e-waste site worker in Accra, Suali. The conversation with Suali confirmed our assumptions as well as informed us of the many other available materials; some as large

as cars. With this knowledge, we revisited Wachusett Watershed to collect materials. We evaluated the condition of the collected items; material composition, working condition, and ease of disassembly. These assessments were used in conjunction with the knowledge gained in the prior sections to evaluate the e-waste materials with the intent of component substitution. With the knowledge of how each component functions, the required properties for each component, the e-waste that is available, and the condition of that e-waste, suggestions for part replacement were made. Using materials from the e-waste site, individual components were substituted into the Stirling engine kit and tested for performance. With each part we collected from the e-waste site in Massachusetts, we discussed them with the Ghana team to gain a broader perspective for the redesign process. We asked them what they thought of our ideas and if they had any additional suggestions for the substitution process. We then began testing parts once we became more confident in how it could fit into the redesign. The tests mainly included temporarily replacing a component with a recycled part on the engine somewhere and running the engine. We would then compare the results from that test with tests where the recycled component was not present to see if it had made a difference. Some recycled parts we found and tested included direct current (DC) motors from a CD player and a toy car, rubber bands of various sizes and thicknesses, various thick metals from computers and other devices, and heat sinks from computer circuit boards.

3.1.3 Co-Design With Academic City University College Students

Co-design was highly integrated into the project and was the main focus in the design and outcome of the process. The Ghana team was consulted and they helped throughout almost all of the steps of the project. They made suggestions to our material selections for substituting parts, they assisted in modeling the computer aided design and received the same engine so that they could be involved in the testing. This process was important for both teams to understand how all of the parts fit together as well as understanding what types of e-waste materials could possibly be used to replace them. Co-design was important for this project because the outcome and final product affects the citizens of Ghana, which is why involving them in the process was essential. Having a Ghana team as partners helps bring the background and knowledge of the community, culture,

and life experiences that differ from our own. The team also partnered with workers at Agbogbloshie. Working with these partners helped gain a deeper insight into the workings of the site. It also provided both teams with valuable information about what materials were available for use for the Ghana team when reconstructing and remodeling the engine out of the e-waste materials. These materials are also accessible to most people living in Accra. Many structural substitutions can be left up to the Ghanaian people who will be recreating the engines for their own personal use. This allows for them to incorporate their own parts and be involved in the making of the engines they will be using. This allows for the design of the engine to be malleable and flexible so that there are many outcomes and possibilities for its design. This helps with the co-design process and allows for the project to be sustainable and long lasting in the area even after the WPI team completes their portion of the work towards the project.

3.2 Ethical Engineering and Method of Data Collection

Ethical engineering is important as the work of engineers has numerous impacts on the quality of life for all people. The role of conducting ethical work is to make it easy for people to trust and value your project. In engineering, there are ethical considerations that must be taken when conducting research and testing. The Code of Ethics for Engineers is a professional guide that all engineers hold each other to follow. The guide outlines standards, duties, and practices to ensure the services engineers provide are honest, impartial, fair, equitable, and safe for all (NSPE, 2019). For the same reason that on a professional level engineers have Code of Ethics to follow and universities have Student Code of Conducts to follow, our team wanted to ensure we safely conducted our work. Although we did not have a written out set of guidelines to follow, we still held each other accountable for our actions and practiced safe methods. As we are working with others outside our group, we respect their choices and rights to not participate if they do not want to. We asked for consent to use their names in the paper which would be published, and in the case of wanting to stay anonymous we respect the rules of confidentiality. All these partners are supporting us in our efforts to complete this project and therefore; we support them in their decisions. This focus on ethical work allows us to work together and make sure all parties are comfortable. All the individuals

we partnered with in this project are given credit for their contributions, whether that be their knowledge, time, finances, or guidance. Without the support from our partners this project would look very different and we must acknowledge those contributions or it would be unfair. It is important to conduct projects ethically to ensure the data and information you are collecting is not wrongfully collected as you want your project to be valued and respected.

3.2.1 Stirling Engine Powered Servomotor and Modeling

An important objective for the MQP is using the Stirling engine to charge cell phones. A selected number of e-waste servomotors were tested and evaluated. The Stirling engine provided the input voltage to the series servomotor to produce an output current that is capable of charging a cell phone for limited amount of use. Generally, alternating current (AC), direct current (DC), brushless DC, gear DC and stepper motors are used to power a number of engines, machines and devices. Power companies supply AC, and in the United States the AC is distributed by alternating sinusoidal voltage and current at frequency of about 60 *herts* and peak voltage of about $\pm$ 120, $\pm$240 *or* $\pm$480 *volts*. An AC motor composes of several nonlinear elements, transitions and variations which make the application of AC motors more complex than a DC motor. A DC motor converts electrical energy into mechanical energy while a DC generator converts mechanical energy into electrical energy. A DC motor is composed of power voltage amplifier, electric circuit, magnetic field coil, brushes and mechanical load. The amplifier supplies voltage to the electric circuit and that voltage supply is then used to generate the field current flowing through the coil of wire. Brushes are attached on the rotating commutator and they act as resistors against the current carrying conductors. Brushes are also noise absorbers and they cause the DC motor to run more quietly. The torque developed by the motor is proportional to the field current and this torque drives the motor shaft. A DC motor can be (a) series configuration, (b) parallel configuration and (c) combined series and parallel configuration. Each configuration provides a different rated torque and speed characteristics. A series configuration is referred to as a series DC motor. This type of DC motors are known to produce torques for a range of speed and load variations as the flow of current increases. Series DC motor are found in

many applications including robotics, medical devices and mining machines. A parallel configuration DC motor is called a shunt motor. In a shunt DC motor there are two or more paths for the current to flow through the circuit elements. The torque produced by the current of one path is independent of the current of the other path. Shunt motors are found in air condition, snow blowers and temperature control fans. The combined series and parallel configurations are called a compound DC motor. In a compound DC motor, the series winding will increase the strengthen of the magnetic field for the shunt winding to response to increasing loads. The amount of speed variation in a compound DC motor depends mainly on the magnetic field strength of the series DC motor. The brushes on the rotating commutator of a DC motor act as resistors against the current carrying conductors and they are also noise absorbers for the DC motor to run more quietly. Gear motors compose of gear boxes which available for reducing speed and torque variations as current flows through the circuit elements. Flywheels, valves, springs, dampers, pulleys, linkages and crank shaft are also available to smooth motor torque and speed variations. The mechanical energy of the Stirling engine from the thermo heat source is stored into the flywheel, and this mechanical energy is refined and transferred to the servomotor through the piston-crank shaft and the driving load. In Figure # the components and assembly of the Stirling engine are depicted.

3.2.2 Formulating Servomotor Equations and Analysis

Direct current motors of series ware widely used a variety of application. These kinds of DC motors are typically equipped with stabilizing circuit devices in order to reduce speed-torque variations as the effective moment of inertia of the rotating components on the output motor shaft is varied The incorporation of a series servomotor into the Stirling engine assembly converts thermo-heat supply to a current-voltage power supply for charging cell phones in Ghana. For the series servomotor, the current flowing through the circuit elements is the same and while the voltage drop across each element in the circuit is different. The input thermo-voltage power by the Stirling engine produces a current to flow through a coil of wires inside the series servomotor. As the current and strength of the magnetic field in the servomotor increase, the difference between the power supply voltage and sum of all the voltage drops across the components of the electric

circuit changes. Figure 16 shows the electric circuit of the servomotor in the Stirling engine assembly. The electric circuit is made up of an applied voltage $v_a(t)$, armature resistance R_a, armature inductance L_a, armature load capacitance C_a, transducer voltage $v_e(\dot{\theta})$ and armature current $i_a(t)$. The purpose of capacitor C_a is to store and release energy at a moment in the Stirling cycle and as required by the voltage difference between the applied voltage $v_a(t)$ and the transducer voltage $v_e(\dot{\theta})$. In the series $R_aC_aL_a$ electric circuit

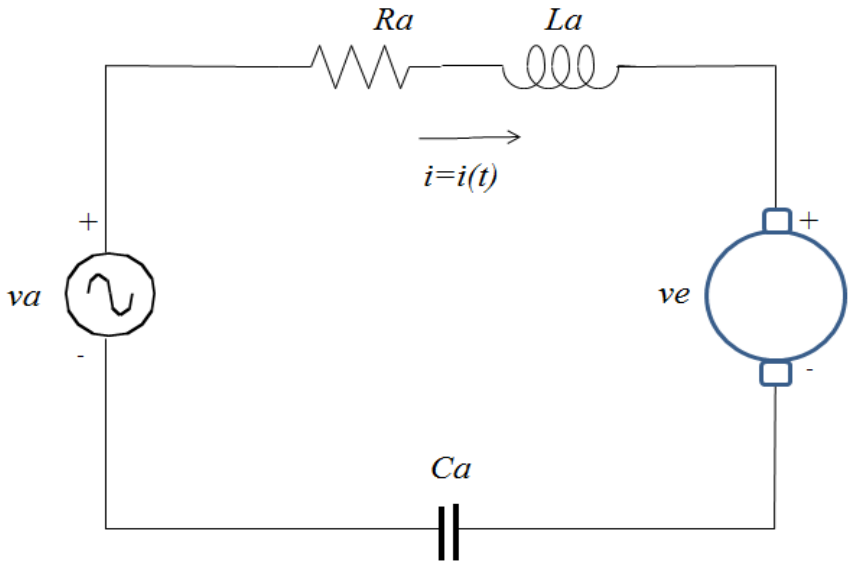

Figure 16: Electric circuit of the armature DC servomotor

it can be seen that the components for the servomotor in the Stirling engine are connected in series with the applied voltage supply $v_a(t)$ and back emf voltage or transducer voltage $v_e(\dot{\theta})$. The transducer voltage $v_e(\dot{\theta})$ is proportional to the angular speed $\omega = \frac{d\theta}{dt} = \dot{\theta}$ of the motor shaft where θ is the motor shaft angle. In addition to the circuit element shown in the Figure # there are the motor shaft angle θ , angular velocity $\omega = \dot{\theta}$, equivalent torsional elastic spring k and bearing and lubricant damper c. Since the applied voltage supply $v_a(t)$ by the Stirling engine, armature current $i_a(t)$, resistance R_a, inductance L_a, load capacitance C_a and voltage transducer $v_e = v_e(\dot{\theta})$ are connected in series, then by

Kirchhoff's Voltage Law (KVL), the applied voltage supply $v_a(t)$ equals to the sum of all the voltage drops across the resistance R_a, inductance L_a, capacitance C_a and transducer voltage $v_e(\dot{\theta})$. Denoting by v_{R_a} the voltage drop across R_a, v_{L_a} the voltage drop across L_a and v_{C_a} the voltage drop across C_a, KVL gives the algebraic equation

$$v_L(t) + v_R(t) + v_C(t) + v_e(\dot{\theta}) = v_a(t), \tag{4}$$

for the series servomotor. Ohms law establishes the relations for the voltage drops in equation (4) in terms of the armature current $i_a(t)$ of the servomotor. In the presence of the resistance R_a, inductance L_a and capacitance C_a in the servomotor, the Stirling engine will produce a current-voltage power supply at speeds proportional to the ratio of L_a to R_a and to the product of R_aC_a. The capacitor in the servomotor is also tuned on based upon the amount of current flow through the terminals and heat loss to the atmosphere. When the capacitor $C_a = 0$, the speed at which the Stirling engine can produce voltage required for charging a cell phone depends upon the ratio of the inductor L_a to the resistor R_a

Current is defined as the time rate of flow of electric charge and mathematically this relationship is written as $i_a = \frac{dq(t)}{dt} = \dot{q}$ where the parameter $q = q(t)$ denotes the electric charge in coulombs. Voltage is measured in volts and current is measured in amperes which is coulombs per second. The servomotor torque $\tau_m(t)$ is proportional to the armature current $i_a = i_a(t)$, and the constant of proportionality k_t is referred to as the torque or servomotor constant. With the current $i_a(t)$ and motor torque constant k_t, we have the torque-current relation $\tau_m(t) = k_t i_a(t)$ that drives all the mass moment of inertia that are mounted on the servomotor shaft. The current, torque and speed of the servomotor are also influenced by the voltage difference $v_a(t) - v_e(\dot{\theta})$. The voltage at the capacitor is defined as $v_{C_a} = \frac{q(t)}{C_a}$ with $C_a \neq 0$. Across the resistance R_a, Ohm's law gives the voltage drop as $v_{R_a} = R_a i(t)$ where the unit of resistance is Ohm which is volt per ampere. Resistance impedes the flow of current and its mechanical engineering analog is damping. The inductance voltage according Ohm's law is proportional to the time rate of change of current and it is written as $v_{L_a} = L_a \frac{di_a}{dt}$ where the inductance L_a is the constant of proportionality. Volt-second per ampere is the unit of the inductance

and this unit is called Henry. Separating the variables in the expression $i_a = \frac{dq(t)}{dt}$ to obtain the differential form $dq = i_a dt$, integrating both sides of this differential form and applying the relation $v_{C_a} = \frac{q(t)}{C_a}$ to the result, yield the Ohm's law for the capacitance

$$v_{C_a}(t) = \frac{1}{C_a}\int_{t_0}^{t} i(t)dt + v_{C_a}(t_0), \quad v_{C_a}(t_0) = \frac{q_0(t_0)}{C_a}, \quad C_a \neq 0, \tag{5}$$

where the initial electric charge $q_0(t_0)$ and initial capacitor voltage $v_C(t_0)$ at the capacitor are values at the initial time t_0. Capacitors are current carrier copper wires and have dimensions of coulomb per volt. One coulomb per volt is equivalent to one Farad. The reciprocal of a capacitor corresponds to an elastic stiffness. Inductance manipulates the rise and fall of a current in the magnetic field and it is measured in henry. Inductance has the dimensions of volt-second per amperes and it corresponds to the mass of a mechanical load. Voltage is the mechanical equivalent of a force, current is equivalent to velocity and electric charge corresponds to displacement. The product of a circuit voltage and current gives the electric power and the rate of change of work is the mechanical power.

Table 1 presents quantities, notations, parameters and terminologies that will appear in the model equations of the servomotor. Also depicted in the table

Table 1. Physical Quantities and Their Notations and Units

quantity	**parameter**	**units**
applied voltage	$v_a = v_a(t)$	*volts*
armature current	$i_a = i_a(t)$	*amperes*
electromotive voltage or transducer voltage	$v_e = v_e(\dot{\theta})$	*volts*
armature resistance	R_a	*Ohms*
armature capacitance	C_a	*Farad*
armature inductance	L_a	*Henrys*
series $R_aC_aL_a$ motor	*current is same*	*voltage is different, KVL*
shunt $R_aC_aL_a$ motor	*current is different*	*voltage is same, KCL*
angular displacement	$\theta = \theta(t)$	*radians*
shaft angular velocity	$\omega = \omega(t) = \dot{\theta}(t)$	*rad/sec*
angular acceleration	$\alpha = \alpha(t) = \ddot{\theta}(t)$	rad/sec^2
motor torque	$\tau = \tau(t) = k_t i_a(t)$	*drived units*
torque/motorconstant	k_t	*derived units*
moment of inertia	J	*drived units*
effective mass	m	*drived units*
effective spring constant	k	*drived units*
effective damping coefficient	c	*derived units*
critical damping coefficient	c_{crit}	*derived units*
undamped natural frequency	ω_n	*rad/sec*
damping ratio	ξ	*dimensionless*

are the effective spring constant k, undamped natural frequency ω_n, effective damping coefficient c, critical damping coefficient c_{crit} and damping ratio ξ. Dimensional analysis is an important way for verifying that the units of quantities are consistent. The SI unit system is also called the MKS system where M is meter, K kilogram and S second.

Centimeter, gram and second (CGS) is another name for the SI system of units. One meter is 100 centimeters and 1×10^6 millimeters equal one kilometer. The dimensions of mass $[M]$, length $[L]$ and time $[T]$ are the MKS dimensions while the foot $[F]$, pound $[P]$ and second $[S]$ are the gravitational dimensions in the USC system. A physical quantity in the notation [.] denotes the dimensions of that physical quantity. The FPS expresses length in feet, weight or force in pounds and time in seconds. Weight has dimensions of $[MLT^{-2}]$ and the expression $m = W/g$ also gives the dimension of the mass. A dimensionless quantity is a quantity without a unit and its dimension is 1. Time is measured in seconds, minutes and hours. One minute is 60 seconds, 60 minutes is one hour and one hour is 3600 seconds. The dimension of time in seconds, minutes and hours is $[T]$. The unit of the arc length of a circle involves length and angle in radian. A radian is the unit of an angle and its dimension is one. A radian is defined as the ratio of the arc length to the radius of the circle making an angle θ with a horizontal axis. One radian is expressed in degrees as $1rad = 360^0/2\pi = 57.3^0$, $1^0 = \pi/180$ and one revolution is 2π radians.

Substituting the expressions of the voltage drops $v_{L_a} = L_a \frac{di_a}{dt}$ for the inductance L_a, $v_{R_a} = R_a i$ for the resistance R_a and $v_{C_a}(t)$ in equation (5) for the capacitance C_a into the KVL algebraic servomotor equation (4) yields the servomotor integral-differential equation

$$L\frac{di(t)}{dt} + Ri(t) + \frac{1}{C}\int_{t_0}^{t} i(t)dt = v_a(t) - v_e(\dot{\theta}) - v_C(t_0). \tag{6}$$

Using the definition $i(t) = \frac{dq(t)}{dt}$, notations $\kappa_{C_a} = 1/C_a$ and $f(t) = v_a(t) - v_e(\dot{\theta}) - v_C(t_0)$, we obtain the second order ordinary differential equation (ODE)

$$L_a\frac{dq^2(t)}{dt^2} + R_a\frac{dq(t)}{dt} + \kappa_C q(t) = f(t), \quad q(t_0) = q_0, \quad \dot{q}(t_0) = v_0, \tag{7}$$

where $\kappa_C = 1/C$ is referred to as the elastance. The initial electrical charge $q(t_0) = q_0$ and current $\dot{q}(t_0) = v_0$ are the values at the initial time t_0. Equation (7) is a second order ODE with constant coefficients and the highest derivative appearing in this ODE is two. Incidentally, there will be two arbitrary constants in the general solution of the second order ODE and the two initial conditions $q(t_0) = q_0$, and $\dot{q}(t_0) = v_0$ are

required to obtain a particular solution. The basic shape of the power supply voltage $f(t) = v_a(t) - v_e(\dot{\theta}) - v_C(t_0)$ of the servomotor can be a constant, variable, sinusoidal and nonlinear functions. The selection of a particular function for the power supply voltage is based upon the voltage supplied by the Stirling engine and speed-torque requirements for driving the loads on the servomotor output shaft.

The servomotor equation (7) is written to a desired standard form by expressing the undamped natural frequency ω_n and damping ratio ξ in terms of the armature resistance R_a, inductance L_a and capacitance C_a. For a mechanical system involving an effective mass m, spring constant k and damping coefficient c, the undamped natural frequency ω_n is defined as $\omega_n = \sqrt{\frac{k}{m}}$, damping ratio is $\xi = \frac{c}{c_{crit}}$ and critical damping $c_{crit} = 2\sqrt{mk} = 2m\omega_n$. These relations correspond to the single degree of mass-dashpot-spring system which is analogous to the electrical R_a, C_a, L_a circuit of the servomotor in the Stirling engine assembly. Diving both sides of the servomotor equation by L_a, setting $\omega_n = \sqrt{\frac{\kappa_C}{L_a}}$, $c_{crit} = 2L_a\omega_n$, $\xi = \frac{c}{c_{crit}} = \frac{R_a}{2\omega_n L_a}$ and simplifying, transform the servomotor equation into the desired standard form

$$\frac{dq^2(t)}{dt^2} + 2\xi\omega_n \frac{dq(t)}{dt} + \omega_n^2 q(t) = \omega_n^2 r(t), \quad q(t_0) = q_0, \quad \dot{q}(t_0) = v_0, \tag{8}$$

where $r(t)$ is the applied voltage and it is now defined as $r(t) = \frac{f(t)}{\kappa_C}$ with $f(t) = v_a(t) - v_e(\dot{\theta}) - v_C(t_0)$. In the servomotor equation (8), the undamped natural frequency $\omega_n^2 = \sqrt{\frac{\kappa_C}{L_a}}$, damping ratio $\xi = \frac{R_a}{2\omega_n L_a}$, applied voltage $r(t)$ and armature current $i_a(t) = \frac{dq(t)}{dt}$ are present. The ratio of the Laplace transform of the applied voltage $r(t)$ to the Laplace transform of the armature current $i_a(t)$ with all the initial conditions in the servomotor being zero is the impedance, denoted by $Z = Z(s)$ and it is a function of the Laplace transform variable s. The Laplace transform variable s is complex number which is contained in the complex space $\mathbb{C}$ and it has real numbers belonging to the real line $\mathbb{R} = (-\infty, \infty)$. The impedance $Z(s) = \frac{\mathcal{L}(r(t))}{\mathcal{L}(i_a(t))} = \frac{R(s)}{I_a(s)}$ of the servomotor in the Stirling engine corresponds to the sum of all the individual impedances in the series circuit configuration where $\mathcal{L}(r(t)) = R(s)$ is the Laplace transform of the applied voltage $r(t)$ and $\mathcal{L}(i_a(t)) = I_a(s)$ is the Laplace transform of the armature current $i_a(t)$. The parameter R_a denotes resistance, inductance L_a, capacitor C_a, voltage input $v_a(t)$ and

current $i_a(t)$. Using the Laplace transform method, the impedance for resistance is $Z_{R_a}(s) = R_a$, inductance is $Z_{La}(s) = L_a s$ and capacitance is $Z_C(s) = 1/C_a s$. In the next section, the definitions and formulas for Laplace and inverse Laplace transforms are presented. Tables of Laplace and inverse Laplace transforms for selected functions are also shown.

3.2.3 Mathematical Methods and Theoretical Analysis

We use the mathematical method of Laplace transform and inverse Laplace transform to obtain solutions for the servomotor ODE (8) and impedance $Z(s) = \frac{\mathcal{L}(r(t))}{\mathcal{L}(i_a(t))} = \frac{R(s)}{I_a(s)}$ with $I_a(s) \neq 0$. Laplace transform deals with the transformation of a piecewise continuous functions $f = f(t)$, and of exponential order on the interval $[0, \infty) \in \mathbb{R} = (-\infty, \infty)$ to a new set of functions $F = F(s)$, $s > 0$ in the complex space $\mathbb{C}$ by means of the definition

$$F(s) = \mathcal{L}(f(t)) = \int_0^\infty e^{-st} f(t) dt = \lim_{\beta \longrightarrow \infty} \left(\int_0^\beta e^{-st} f(t) dt \right), \tag{9}$$

for all values of $s > 0$ such that the limit of the proper integral exists. The notation $F(s) = \mathcal{L}(f(t))$ denotes the Laplace transform of the original function $f(t)$, $t \geq 0$ and s is the frequency domain variable. The time domain variable $t \in \mathbb{R}$ is a real number while $s \in \mathbb{C}$ is a complex number. A number written as the form $s = \sigma + j\omega$ is called a complex number, where $j = \sqrt{-1}$ is referred to as the imaginary unit, σ is the real part and ω is the imaginary part. The number $\bar{s} = \sigma - j\omega$ is called the complex conjugate of $s = \sigma + j\omega$ and the multiplication of these two complex numbers $s = \sigma + j\omega$ and $\bar{s} = \sigma - j\omega$ yields the result $(\sigma + j\omega)(\sigma - j\omega) = \sigma^2 + \omega^2$. We think of the exponential function e^{-st} in equation (9) as a weighting function that slows down the growth rate of $f(t)$ for $t \geq 0$ where the base e for $-st$ is the base for the natural logarithm of $\ln e^x = x$. To determine $F(s) = \mathcal{L}(f(t))$, we integrate the proper integral as t varies from 0 to β and then take the limit of the derived result as $\beta \longrightarrow \infty$. Integration from 0 to ∞ is referred to as improper integral. Capital letters are typically used to denote the Laplace transform of a function. The Laplace transform of the functions $f(t)$, $v_a(t)$ and $i_a(t)$ are $\mathcal{L}(v(t)) = F(s)$, $\mathcal{L}(v_a(t)) = V_a(s)$ and $\mathcal{L}(i_a(t)) = I_a(s)$, respectively. Laplace transformed functions in terms of the Laplace transform variable s are called frequency functions

and they are expressed in the frequency domain. The functions depending upon the time t are called time functions and they are defined in the time domain. The Laplace transform is also an important method for solving differential equations with constant coefficients. This method enables one to solve differential equations together with the initial conditions without going through multiple solution steps.

The Laplace transform and Inverse Laplace transform methods are used to obtain explicit expressions for the servomotor current $i_a(t)$, torque $\tau_m(t) = k_t i_a(t)$ and voltage power supply for the charging system. Units of quantity measure are not typically assigned to Laplace transformed expressions depending upon the Laplace transform variable. The impedance $Z(s)$ is a transfer function of a linear electric circuit and it is defined as the ratio of the Laplace transform of the voltage to the Laplace transform of the current with all the initial conditions in the electrical circuit being zero. The inverse Laplace transform is the process of converting the frequency function $F(s)$ in terms of the Laplace transform variable s to the time function $f(t)$. This is achieved by using the formula

$$f(t) = \mathcal{L}^{-1}(F(s)) = \frac{1}{2\pi j} \int_{\sigma - j\infty}^{\sigma + j\infty} F(s) e^{st} ds, \quad s \in \mathbb{C}, \quad t \in \mathbb{R}, \tag{10}$$

for which routine algebra cannot easily produce the inverse Laplace transform$\mathcal{L}^{-1}(F(s))$ of $F(s)$. In the Laplace transform formula (9), the notation $\mathcal{L}(f(t))$ donates the Laplace transform of the time function $f(t)$ and in the formula (10) for the inverse Laplace transform, the notation $\mathcal{L}^{-1}(F(s))$ represents the inverse Laplace transform of $F(s)$. Admittedly, using the formula (10) to find the inverse Laplace transform of $\mathcal{L}^{-1}(F(s)) = f(t)$ is not a straight forward calculation. We often rely on the use of tables of Laplace and inverse Laplace transforms. Tables 2, 3 and 4 show a number of selected functions and their corresponding Laplace and inverse Laplace transforms. Partial fraction expansion and algebraic simplifications play a major role in finding a match of frequency functions in the Tables of Laplace and inverse Laplace transforms.

In this table

Table 2. Constant, Polynomial and Impulsive Functions

Typical Functions	**Time Functions** $f = f(t),\ t \geq 0$	**Frequency Functions** $F(s) = \mathcal{L}(f(t)),\ s > 0$
formula	$\mathcal{L}(f(t)) = \int_0^\infty e^{-st} f(t)dt,$	$F(s)$
homogenous	$cf(t),\ c = [c_1, c_2] \in \mathbb{R}$	$cF(s)$
linearity	$c_1 f_1(t) \pm c_2 f_2(t)$	$c_1 F_1(s) \pm c_2 F_2(s)$
unit step	1	$\frac{1}{s}$
unit ramp	t	$\frac{1}{s^2} = \frac{1}{s}\mathcal{L}(1)$
parabolic	t^2	$\frac{2}{s^3} = \frac{2}{s}\mathcal{L}(t)$
cubic	t^3	$\frac{6}{s^4} = \frac{3}{s}\mathcal{L}(t^2)$
$n-$polynomial	$t^n,\ n = 1, 2, 3, ...$	$\frac{n!}{s^{n+1}}$
$n-1-$polynomial	$\frac{1}{(n-1)!}t^{n-1},\ n = 1, 2, 3, ...$	$\frac{1}{s^n}$
$k-1-$polynomial	$\frac{1}{\Gamma(k)}t^{k-1},\ k = 1, 2, 3, ...$	$\frac{1}{s^k}$
unit impulse	$\delta(t)$	1
shifting impulse	$\delta(t-a)$	e^{-as}
shifting impulse	$\delta(t-1)$	e^{-s}
shifting impulse	$\delta(t-2)$	e^{-2s}
shifting impulse	$\delta(t-3)$	e^{-3s}

constant, impulse and polynomial functions, which are typically used to describe the shapes of the voltage and current in a servomotor are transformed from time domain variable to a frequency domain variable. The use of the Laplace transform tables provides a convenient way to obtain the inverse Laplace transform $f(t) = \mathcal{L}^{-1}(F(s))$ without the use of improper integration formula (10). Pairs of time functions and $s-$dependent functions $F(s)$ are available in the Laplace transform table. The Laplace transform of an applied unit voltage to the Stirling engine is $\mathcal{L}(1) = F(s) = 1/s$. If the applied voltage to the Stirling engine is the unit ramp function $f(t) = t$, then its Laplace transform

$\mathcal{L}(t)$ is $F(s) = 1/s^2$. The Laplace transform of the delta or impulse voltage function $f(t) = \delta(t)$ is $\mathcal{L}(\delta(t))$ is $F(s) = 1$. The inverse Laplace transform $\mathcal{L}^{-1}(1)$ is the delta or impulse function $\delta(t)$. When the frequency function $F(s) = s$, the inverse Laplace transform $\mathcal{L}^{-1}(s)$ is $\mathcal{L}^{-1}(s) = \frac{d\delta(t)}{dt}$, and for $F(s) = s^2$, the inverse Laplace transform is $\mathcal{L}^{-1}(s^2) = \frac{d^2\delta(t)}{dt^2}$. In Table 3

Table 3. Exponential, Sinusoidal and Special Functions

Typical Functions	**Time Functions** $f = f(t),\ t \geq 0$	**Frequency Functions** $F(s) = \mathcal{L}(f(t)),\ s > 0$
growth exponential	$e^{at},\ a > 0$	$\frac{1}{s-a},\ s \neq a$
decay exponential	$e^{-at},\ a > 0$	$\frac{1}{s+a},\ s \neq -a$
multiplicative	$te^{at},\ a > 0$	$\frac{1}{(s-a)^2},\ s \neq a$
multiplicative	$te^{-at},\ a > 0$	$\frac{1}{(s+a)^2},\ s \neq -a$
multiplicative	$t^n e^{-at},\ n = 1, 2, 3, ...$	$\frac{n!}{(s+a)^{n+1}},\ s \neq -a$
multiplicative	$\frac{1}{(n-1)!}t^{n-1}e^{at}$	$\frac{1}{(s-a)^n},\ s \neq a$
gamma function	$\frac{1}{\Gamma(k)}t^{k-1}e^{at},\ k > 0$	$\frac{1}{(s-a)^k},\ s \neq a$
cosine	$\cos \omega t$	$\frac{s}{s^2+\omega^2},\ s^2 + \omega^2 \neq 0$
sine	$\sin \omega t$	$\frac{\omega}{s^2+\omega^2},\ s^2 + \omega^2 \neq 0$
damped cosine	$e^{-at}\cos \omega t$	$\frac{s+a}{(s+a)^2+\omega^2},\ (s+a)^2 + \omega^2 \neq 0$
damped sine	$e^{-at}\sin \omega t$	$\frac{\omega}{(s+a)^2+\omega^2},\ (s+a)^2 + \omega^2 \neq 0$
excited cosine	$t\cos \omega t$	$\frac{s^2-\omega^2}{(s^2+\omega^2)^2},\ s^2 + \omega^2 \neq 0$
excited sine	$t\sin \omega t$	$\frac{2\omega s}{(s^2+\omega^2)^2},\ s^2 + \omega^2 \neq 0$
hyperbolic cosine	$\cosh \omega t$	$\frac{s}{s^2-\omega^2},\ s^2 - \omega^2 \neq 0$
hyperbolic sine	$\sinh \omega t$	$\frac{\omega}{s^2-\omega^2},\ s^2 - \omega^2 \neq 0$

the Laplace transforms of exponential, sinusoidal and hyperbolic functions are presented. The Laplace transform expressions in both Tables 2 and 3 are obtained using the formula equation (9) of the Laplace transform. The algebraic properties involved in the definitions of Laplace and inverse Laplace transforms further simplify the collection of functions for the Laplace transform tables. According to the final value theorem, the Laplace transform

and inverse Laplace transform are related by the expression $\lim_{t\longrightarrow\infty} f(t) = \lim_{s\longrightarrow 0} sF(s)$ which can determine the growth and decay rates of the circuit voltage and currents of the servomotor. The initial values for the circuit elements of the servomotor can be quantified using the initial value theorem $\lim_{t\longrightarrow 0} f(t) = \lim_{s\longrightarrow\infty} sF(s)$ connecting the Laplace and inverse Laplace transforms. Again using the Laplace transform formula (9), the Laplace transformed expressions for selected differential, integral and convolution functions are shown in Table 4

Table 4. Differential, Integral and Convolution Functions

Typical Functions	**Time Functions** $f = f(t),\ t \geq 0$	**Frequency Functions** $F(s) = \mathcal{L}(f(t)),\ s > 0$
$1st-$derivative	$f^{'}(t)$	$sF(s) - f(0)$
$2nd-$derivative	$f^{''}(t)$	$s^2F(s) - sf(0) - f^{'}(0)$
$3th-$derivative	$f^{'''}(t)$	$s^3F(s) - s^2f(0) - sf^{'}(0) - f^{''}(0)$
$nth-$derivative	$f^{(n)}(t)$	$s^nF(s) - s^{n-1}f(0) - s^{n-2}f^{'}(0) - .....- f^{(n-1)}(0)$
multiplication	$tf(t)$	$-F^{'}(s),\ F(s) = \mathcal{L}(f(t))$
multiplication	$-tf(t)$	$F^{'}(s),\ F(s) = \mathcal{L}(-f(t))$
multiplication	$t^2f(t)$	$F^{''}(s) = \frac{d^2F(s)}{ds^2}$
multiplication	$t^nf(t)$	$(-1)^nF^{(n)}(s),\ F^{(n)}(s) = \frac{d^nF}{ds^n}$
multiplication	$te^{at},\ a > 0$	$-\frac{d}{ds}\left(\frac{1}{s-a}\right) = \frac{1}{(s-a)^2},$
multiplication	$te^{-at},\ a > 0$	$-\frac{d}{ds}\left(\frac{1}{s+a}\right) = \frac{1}{(s+a)^2}$
multiplication	$-te^{-at},\ a > 0$	$\frac{d}{ds}\left(\frac{1}{s+a}\right) = -\frac{1}{(s+a)^2}$
multiplication	$-t\cos\omega t$	$\frac{d}{ds}\left(\frac{s^2-\omega^2}{(s^2+\omega^2)^2}\right)$
multiplication	$-t\sin\omega t$	$\frac{d}{ds}\left(\frac{2s\omega}{(s^2+\omega^2)^2}\right)$
integration	$\int f(t)dt$	$\frac{F(s)}{s} \_ \frac{f(0)}{s}$
convolution	$(f*g)(t) = \int_0^t f(\tau)g(t-\tau)d\tau = \int_0^t f(t-\tau)g(\tau)d\tau$	$\mathcal{L}(f*g) = \mathcal{L}(f)\mathcal{L}(g)$

For the armature current $i_a(t)$ of the servomotor, the voltage drop v_{R_a} across the armature resistance R_a is described by $v_{R_a}(t) = R_a \frac{dq(t)}{dt}$ and its Laplace transform is $\mathcal{L}(v_{R_a}(t)) = R_a(sQ(s) - q(t_0)$ where $q(t_0)$ is the initial electric charge at the time $t = t_0$. The Laplace transform of the voltage drop at the inductance $v_{L_a}(t) = L_a \frac{d^2q(t)}{dt^2}$ is $\mathcal{L}(v_{L_a}(t)) = L_a(s^2Q(s) - sq(t_0) - \dot{q}(t_0))$ where $\dot{q}(t_0)$ is the initial current in the electric circuit of the servomotor. The inverse Laplace transform of the circuit current $I_a(s) = sQ(s) - q(t_0)$ of the servomotor is $\mathcal{L}^{-1}(I_a(s)) = \frac{dq(t)}{dt}$.The expressions in Tables 2, 3 and 4 of Laplace transforms are helpful in solving ODEs involving constant coefficients, first, second or higher order derivative functions.

CHAPTER 4. RESULTS AND DISCUSSION

4. Introduction

The following section is an accumulation of the data collected and the results of the calculations and tests performed throughout the project. We start with the data collected from measuring the components of the Stirling engine kit and the resulting SolidWorks drawings. From there we provide the results of the tests performed relating to the different temperatures and environments the Stirling engine was tested in. Next, we include the data collected from testing the revolutions per minute of the flywheel. We then review the results of the tests performed on the e-waste materials.

4.1 Guidelines for Selecting and Using E-Waste Materials

The guidelines for selecting and replacing the components of the Stirling engine with e-waste materials are drawn from our engineering design iterations, testing and analysis. Admittedly, these guidelines will reduce the manual effort and cost burden of the unstructured ways of managing e-waste in Ghana. The Co-design activities and interviews with the students and professors at Academic City University College in Ghana further suggested that the proposed guidelines will bring about a structural shift for an increased e-waste economy. The voltage generated by the Stirling engine with an e-waste servomotor in the assembly was between 4.8 volts and 5 volts. Our laboratory tests and analysis quantified this required voltage for charging cell phone in Ghana's remote places. The e-waste site in Agbogbloshie, Ghana is consistent with what is seen in many other e-waste sites in Sub-Saharan Africa. There are several factors that account for the large variations of e-waste in Ghana and other African countries. From political incentives to business opportunities for more productive uses of e-waste are some of the factors driving the quantities, weight and variety of e-waste in communities across in Ghana. Combined interviews with our partners in Ghana, research and analysis indicated the variety of e-waste, especially computers, laptops, televisions, mobile phones, printers and many other bulky electronics that are available in Ghana. The proposed guidelines as described in the MQP report will provide a background of greater awareness about more productive uses of e-waste, toxic substances that harm health and the environment and safety practices for e-waste workers. It is conceivable to use the guidelines to create

e-waste trade codes, strengthen e-waste regulations and practical methods for disposing end of life e-waste products.

4.1.1 Initial Component Measurements and Drawings

The team began collecting data on the original Stirling engine to better understand the components involved in the engine. This includes data collection for each individual part in the engine and is presented as a bill of materials and the dimensions of the parts which can be found in Appendix B and Appendix C respectively. The engine was disassembled so the mass of each individual part could be measured. From there the mass of each sub assembly and the full Stirling engine was found. The team performed a series of tests on the original Stirling engine to assess the functionality and efficiency of the engine. The purchased Stirling engine was advertised with the ability to reach an output voltage range of five to nine volts. When the heat was first applied to the hot cylinder of the engine, the highest output voltage reached was approximately 2.6V. The team then made adjustments to the length of the piston arm on the cold cylinder of the engine. The length was changed by adjusting where the pin of the flywheel was attached to the piston arm as shown in Figure 17. In this figure

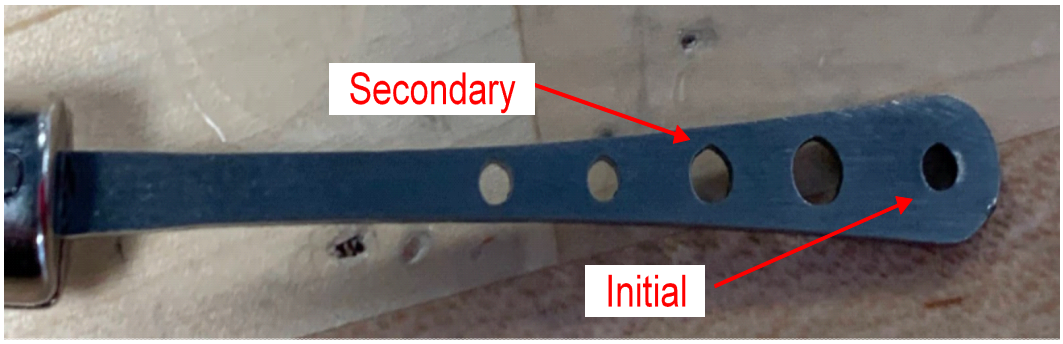

Figure 17: Piston arm with indicated length adjustmen

the initial and secondary holes for the adjustments are depicted. We started with adjusting it by one hole difference which was approximately 0.18 inches, leading to an increase of about one volt. The engine was running at about 3.6V after this change. Unfortunately, the next hole on the piston arm was not cut large enough for the pin, so the team instead adjusted the length of the arm on the hot-cylinder piston. The adjustment to the

piston in the piston connector decreased the volume in the hot cylinder; this increased the voltage. This increase was due to the rise in pressure in the hot cylinder which resulted in a greater difference between the hot and cold cylinder pressures. This adjustment also decreased the fluid in the hot cylinder that needed to be heated up, which allowed it to heat up faster, therefore increasing the output speed of the flywheels which in turn increased the output voltage.

The new engine that was purchased was able to produce six volts of output. When the engine reached this voltage the team attached a cell phone to see results. The phone was able to recognize the voltage and indicated that it began to charge. Shortly after, the resistance caused by the phone made the voltage output drop to 3.8V. The phone then stopped charging. To keep the cell phone charging, the Stirling engine must maintain a five volt reading or higher when the phone is connected. Due to the drop in voltage from the resistance, we were unable to get the cell phone to charge consistently with the open flame as a heat source. From a suggestion made by our advisor, we performed a few tests on the engine with a more direct heat source; a torch. This was to test if the engine could produce a higher voltage with a consistent heat source. The torch was lit and held about eight to nine inches away from the hot cylinder, and with a gentle push of the flywheel the engine started running. It reached its maximum voltage within less than a minute, faster than all other trials, and had the highest reading out of any previous runs of 7.4V. We connected a cell phone in and it began charging and even with the resistance, which caused the voltage to drop to five volts, the phone continued charging.

4.1.2 Temperature and Environment Testing

In order to test the Stirling engine's ability to charge a cell phone or a battery to charge a cell phone, the team conducted a series of tests and calculations. The team identified that the surrounding temperature of the Stirling engine could have significant effects on the voltage output and the efficiency of the engine.

The team tested the following factors at different temperatures:

- Maximum voltage
- Time for the engine to start after igniting the flame
- Time to reach maximum voltage

• Time to stop after extinguishing the flame

Figures 17, 18, 19, and 21 are the graphs of the results for these measurements from the original engine. Additional information can be found in Appendix C. In this graph

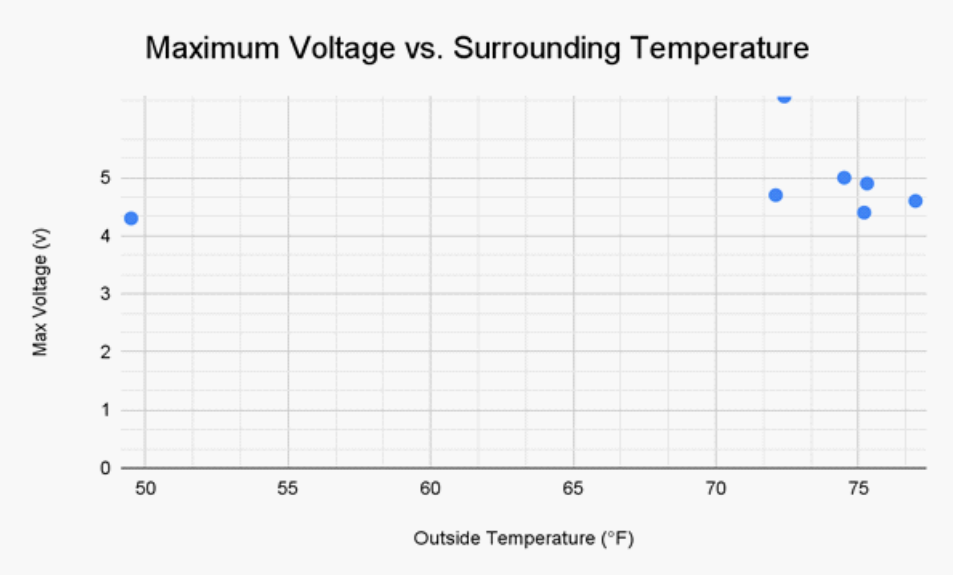

Figure 18: Graph of maximum voltage versus surrounding temperature

the points are scattered and mostly concentrated on a region for the temperature greater than $70^0 F$.

We have similar situation in the subsequent graphs

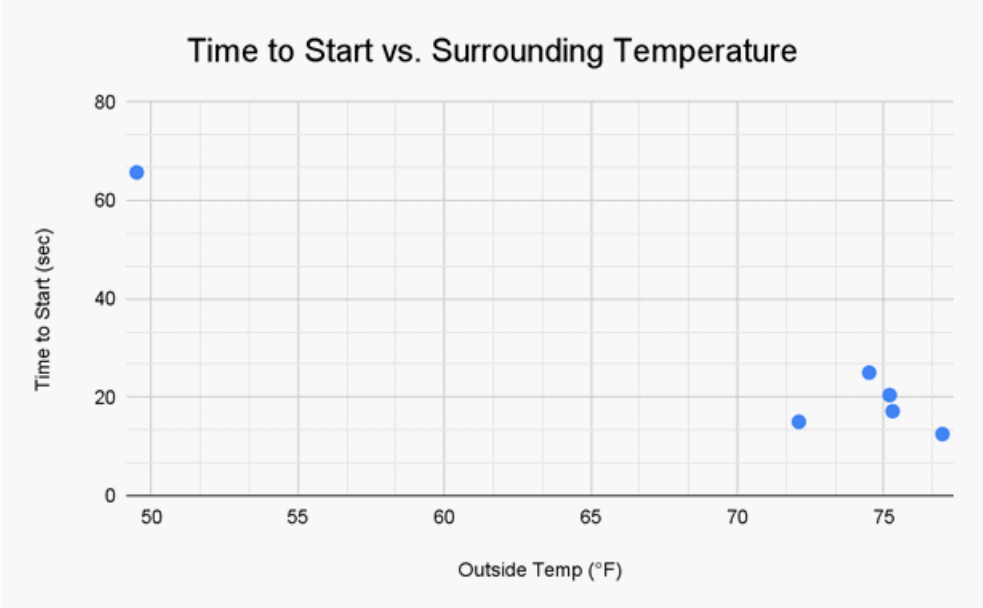

Figure 19: Graph of the time to start the engine versus differing surrounding temperature

These tests showed that the room temperature the engine is run in can affect the efficiency of the engine. When the temperature was run in very cool temperatures of 49.5 °F, the time to start the engine was significantly higher than when the temperature was 70°F and higher. We believe this is because the hot cylinder is cooler at the start, causing it to take longer to reach a temperature that is hot enough to create the pressure difference that allows for the engine to run. There does not appear to be any significant change in efficiency of the engine when the temperature only differs by a few degrees. Based on observation, after the engine runs for multiple iterations of the tests the efficiency decreases. The team theorized that this decrease in efficiency correlates to the decrease in temperature difference between the two cylinders. The flame's heat that is applied to the hot cylinder is also being applied to the cold cylinder due to their proximity. The team started to look into the application of heat sinks on the engine as pictured in Figure 22.

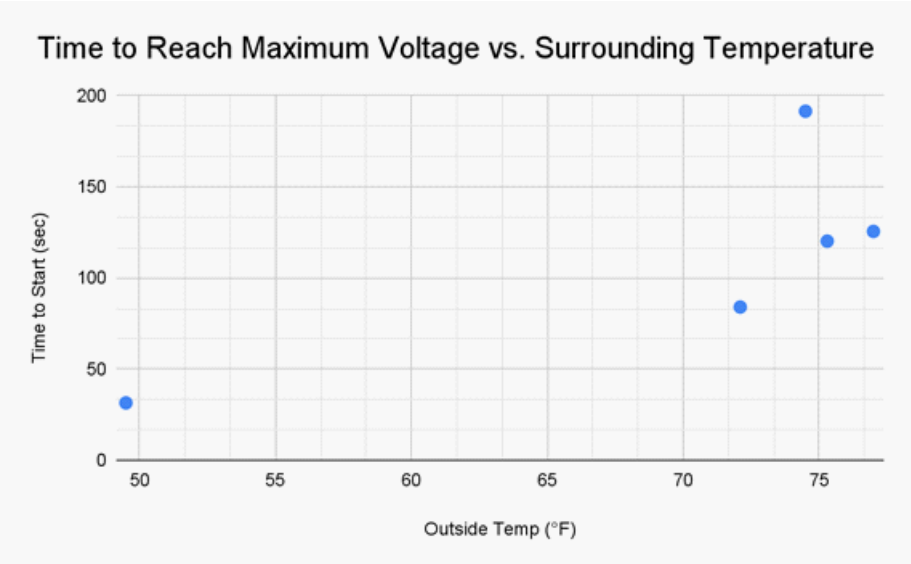

Figure 20: Graph of time to reach the maximum voltage versus surrounding temperature

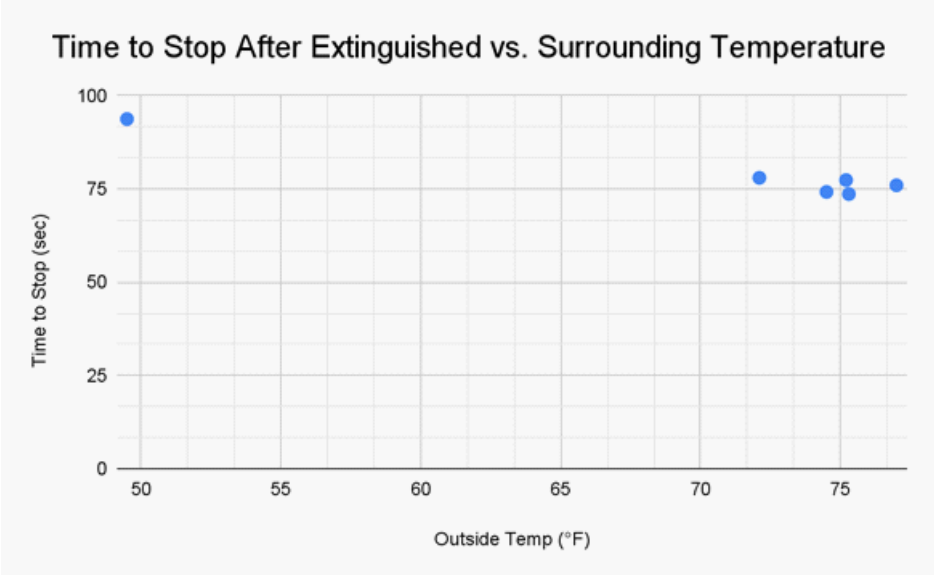

Figure 21: Graph of time to stop after extinguished versus differing surrounding temperature

We use the Stirling engine in this figure

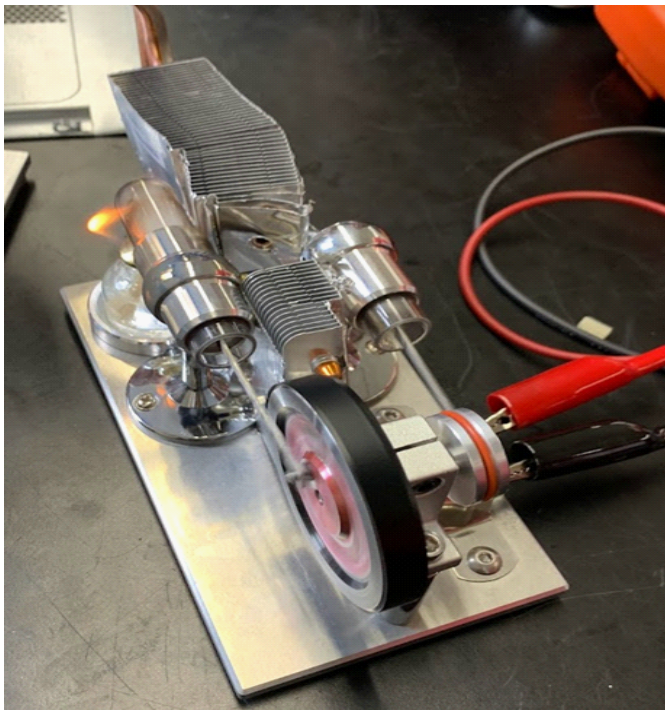

Figure 22: Stirling Engine with recycled heat sinks applied between the hot and cold

to conduct more tests for a proper conclusion to be made but based on preliminary tests it seems that the heat sinks create a barrier between the flame and the cold cylinder and increase the voltage output by a few decimals of voltages. Additional data from the heat sink test can be found in Appendix C.

4.1.3 Flywheel Speed and Waste Test Results

The flywheel speed was found to have inconsistent results. As shown in the graph in Figure 23, the results of the speed readings were drastically different for the same voltage outputs. This is inconsistent with the calculations of revolutions per minute correlating to voltage output, for they should have similar readings. The team believes this is due to an error with the tachometer that we used which had imprecise and inconsistent readings. The result could have been affected by the reflective material of the flywheel as well. The tachometer runs by shining a laser off of a reflective piece of tape, however, since the entire Stirling engine is reflective the device was likely picking up inconsistent readings. After applying black out tape to the flywheel, the readings were still not accurate. Below

is the graph showing the range of results. Additional data for the graph

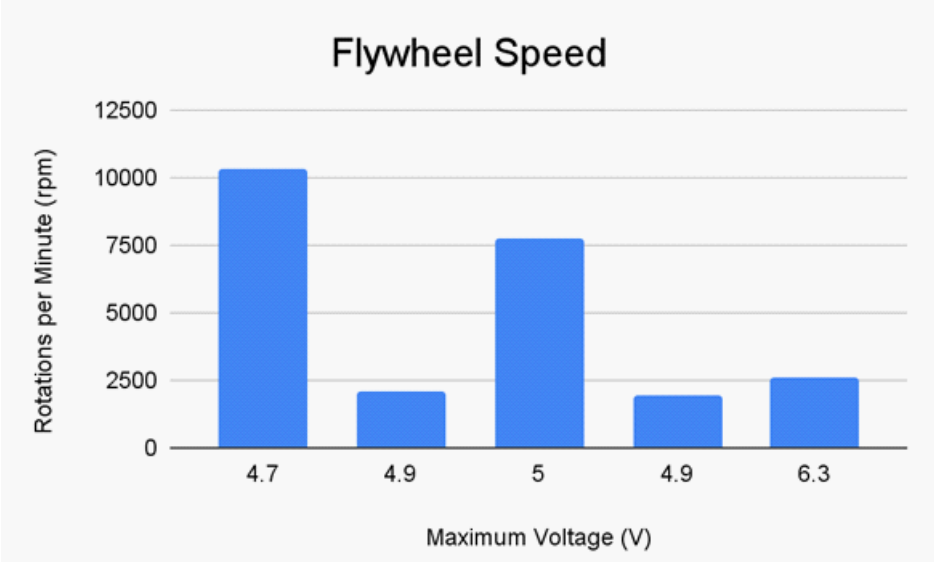

Figure 23: Graph of the rotations per minute versus maximum voltage

can be found in Appendix C.

With regards to the selection and replacement of the Stirling components with e-waste, the team tested the functionality of the e-waste material to identify its ability to replace parts of the engine. These tests included functionality tests as well as efficiency tests. The tests were to ensure the capabilities of the e-waste parts. The parts that we tested were motors, heat sinks, and elastic bands. The team found motors from a used CD player and from a toy car. The test done on the motor was purely for functionality. The team replaced the motor on the original Stirling engine with the e-waste motors to assess their performance.

The team replaced each motor one by one and tested to see if they were able to produce an output voltage; Figure 24 displays the results. Additional information for the graph

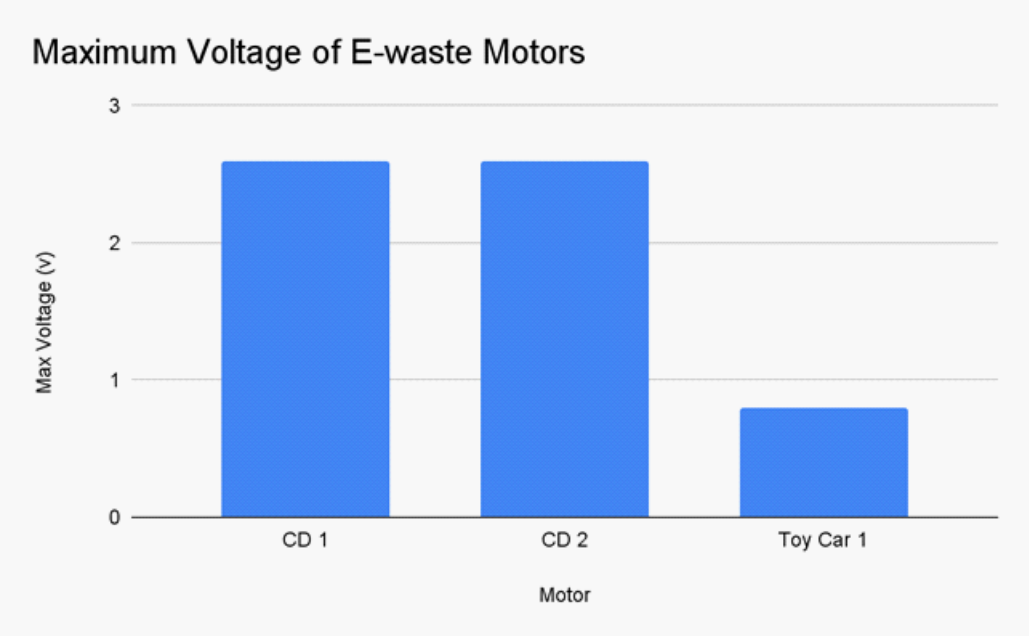

Figure 24: The max voltage of different e-waste motors

can be found in Appendix C.

The output voltage that was produced by the recycled motors reached a maximum of about half the output voltage required to charge a cell phone. Due to a malfunction during the testing of the toy car engine the team observed, further observation and calculations were needed. While testing the toy car engine it took significantly longer for the engine to reach the necessary starting temperature, and when the engine did start it had a much lower voltage output then any of the motors we had previously tested. The team assumed the low voltage was because this was an old, used engine. This problem was solved during one test when the belt attaching the cold cylinder flywheel and the motor flywheel became misaligned and slipped off. When this occurred the engine seemed to significantly increase in speed. This is most likely due to the toy car motor having a significantly higher resistance than that of any other motor that the team had previously tested.

4.2. Servomotor and Stirling Engine Performance Analysis

We want to find values for the circuit elements R_a, C_a, L_a of the servomotor for which the required voltage to charge a cell phone is produced. In addition to locating specific values for the parameters R_a, C_a and L_a, the time and speed required to produce a voltage near or equal to 5 volts are also of interest for replacing the Stirling engine components with e-waste materials. The time and speed for producing the current and voltage for the proposed charging system are determined by suppling constant heat source to the Stirling engine. Taking term by term Laplace transform of the servomotor equation (8) and simplifying the algebra lead to the electric charge

$$Q(s) = \frac{(s + 2\xi\omega_n)q_0 + v_0}{s^2 + 2\xi\omega_n s + \omega_n^2} + \frac{\omega_n R(s)}{s^2 + 2\xi\omega_n s + \omega_n^2}, \quad R(s) = \frac{1}{\kappa_C}\mathcal{L}(f(t)), \tag{11}$$

which is now a function of the Laplace transform variable s and $\mathcal{L}(f(t)) = \mathcal{L}(v_a(t) - v_e(\dot{\theta}) - v_C(t_0))$. The quantities q_0 and v_0 are the initial values in the servomotor. In this servomotor equation $\mathcal{L}(q(t)) = Q(s)$ and $\mathcal{L}(r(t)) = \frac{1}{\kappa_C}\mathcal{L}(f(t)) = R(s)$. On the left hand side of the electric charge function $Q(s)$, the rational expression containing the initial conditions q_0 and v_0 is referred to as the complementary function or transient function. For given initial values for q_0 and v_0, the growth and decay rates of the armature current $i_a(t)$ of the servomotor can be determined as the damping ratio $\xi = \frac{R_a}{2\omega_n L_a}$ and undamped natural frequency $\omega_n = \sqrt{\frac{\kappa_C}{L_a}}$ are varied. The growth and decay rates are separated from each other when damping coefficient $c = R_a$ and critical damping $c_{crit} = 2\sqrt{L_a\kappa_C} = 2L_a\omega_n$ are identical The rational expression containing the applied voltage $R(s)$ in equation (11) is called the particular function or the steady state function. The inverse Laplace transform of both the transient and steady state functions of $Q(s)$ gives the electric charge $q(t)$, the armature current $i_a(t)$ and corresponding voltage drops $v_{L_a}(t)$ for the inductance L_a, $v_{R_a}(t)$ for the resistance R_a and $v_{C_a}(t)$ for the capacitance C_a.

4.2.1. Characteristic Equation and Poles of the Servomotor

Applying the Laplace transform method to the servomotor equation (8) gives frequency function $Q(s)$ for the electric charge as seen in equation (11). This frequency function of $Q(s)$ is a function of the Laplace transform variable s and it composes of the circuit elements R_a, C_a, L_a. The transient and steady state frequency functions for the electric charge $Q(s)$ are infinity for values of s satisfying the characteristic equation

$$D(s) = s^2 + 2\xi\omega_n s + \omega_n^2 = 0, \tag{12}$$

where $\xi = \frac{R_a}{2\omega_n L_a}$, $\omega_n = \sqrt{\frac{\kappa_C}{L_a}}$ and $\kappa_C = \frac{1}{C_a}$, $C_a \neq 0$. Roots and poles are typical names for the values of s satisfying the characteristic equation $D(s) = 0$. Using the well known quadratic formula for solving the standard quadratic equation $ax^2+bx+c = 0$, we obtain the poles

$$s_1 = -\xi\omega_n + \omega_n\sqrt{\xi^2 - 1}, \quad s_2 = -\xi\omega_n - \omega_n\sqrt{\xi^2 - 1}, \tag{13}$$

of the servomotor. for the discriminant $\Delta = \xi^2 - 1 > 0$. The poles s_1 and s_2 are located on the real line in the left hand side of the complex plane. In the complex plane, the vertical axis is designated as the imaginary axis and the horizontal axis is the real axis. The complex index $j = \sqrt{-1}$ is marked on the vertical axis of the complex plane. Denoting the discriminant Δ by $\Delta = \xi^2 - 1$, maintaining the undamped frequency $\omega_n = \sqrt{\frac{\kappa_C}{L_a}}$ as a constant and and varying the damping ratio $\xi = \frac{R_a}{2\omega_n L_a}$, the poles of the characteristic equation $D(s) = 0$ will change. In essence, as the discriminant $\Delta = \xi^2 - 1$ changes, the poles of the characteristic equations $D(s) = 0$ can be real and distinct poles, real and repeated poles, or occur in complex conjugate poles of the form $s_{1,2} = \sigma \pm j\omega$ where the real part $\mathrm{Re}(s_{1,2}) = \sigma$ and imaginary part $\mathrm{Im}(s_{1,2}) = \omega$.

4.2.2 Servomotor and Stirling Engine Performance

The complex conjugate poles $s_{1,2} = \sigma \pm j\omega$ with $\sigma = -\xi\omega_n$ and $\omega = \omega_n\sqrt{1 - \xi^2}$ when discriminant $\Delta = \xi^2 - 1 < 0$. For any value of $\xi = \frac{R_a}{2\omega_n L_a}$ in the open interval $(0, 1)$ of the real line $\mathbb{R} = (-\infty, \infty)$ the performance the servomotor is asymptotically stable by Lyapunov sense, and the Stirling engine generate more armature current than the case when $R_a > 2\omega_n L_a$. Concrete values for the armature resistance R_a, armature inductance L_a and armature capacitance C_a of the servomotor of the Stirling engine can

be selected in such way that the damping ratio ξ satisfies the inequality $0 < \xi < 1$ and for a fixed undamped natural frequency $\omega_n = \sqrt{\frac{\kappa_C}{L_a}}$. As the time t approaches to infinity, the armature current $i_a(t)$ decays exponentially. The torque driving the moment of inertia of the loads on the servomotor output shaft will also decay exponentially as $t \to \infty$. When the discriminant $\Delta = \xi^2 - 1 = 0$, the damping ratio $\xi = \frac{R_a}{2\omega_n L_a} = 1$. This is referred to as the critical case that distinguishes regions of slow and fast performance of the servomotor and the Stirling engine. The poles s_1 and s_2 of the characteristic equation $D(s) = 0$ are real and equal. Incidentally, the values of the armature resistance R_a and inductance L_a of the servomotor are also equivalent. When the armature resistance R_a of the servomotor is zero, the regions of stable and unstable performance of the servomotor of the Stirling engine are established. In the unstable region, the armature current $i_a(t)$ and torque $\tau_m = k_t i_a(t)$ of the servomotor will grow exponentially as $t \to \infty$ and while in the stable region, these physical quantities will decay exponentially as $t \to \infty$. In the unstable region, the charging of cell phones with the current generated by the Stirling engine will experience interruptions. There will also be persistent breakdowns in the flow of the armature current $i_a(t)$ into the cell phone chargers. The problem causing the instability in the current flow into the cell phone chargers should be fixed first and then resume the charging of the cell phones using the Stirling engine. For the discriminant $\Delta = \xi^2 - 1 > 0$, the damping ratio $\xi = \frac{R_a}{2\omega_n L_a} > 1$ and the poles of the characteristic equation $D(s) = 0$ are $s_1 = -\xi\omega_n + \omega_n\sqrt{\xi^2 - 1}$ and $s_2 = -\xi\omega_n - \omega_n\sqrt{\xi^2 - 1}$. This is the case when concrete values for the armature inductance L_a must satisfy the inequality $0 < L_a < \frac{R_a}{2\omega_n}$ and with $\omega_n = \sqrt{\frac{\kappa_C}{L_a}} \neq 0$. Although both the armature current $i_a(t)$ and torque $\tau_m = k_t i_a(t)$ of the servomotor will decay exponentially as the time $t \to \infty$, the performance of the Stirling engine is slower than the case when the damping ratio satisfies the inequality $0 < \frac{R_a}{2\omega_n L_a} < 1$. Setting the voltage difference $v_a(t) - v_e(\theta) - v_{C_a}(t_0) = 0$

will yield $R(s) = 0$ in equation (11) and the expression for transient electric charge

$$\begin{aligned} Q_{trs}(s) &= \frac{(s+\xi\omega_n)q_0 + v_0 + \xi\omega_n q_0}{s^2 + 2\xi\omega_n s + \omega_n^2} \\ &= \frac{(s+\xi\omega_n)q_0}{s^2 + 2\xi\omega_n s + \omega_n^2} + \frac{v_0 + \xi\omega_n q_0}{s^2 + 2\xi\omega_n s + \omega_n^2} \\ &= \frac{(s+\xi\omega_n)q_0}{(s+\xi\omega_n)^2 + \omega_n^2(1-\xi^2)} + \frac{v_0 + \xi\omega_n q_0}{(s+\xi\omega_n)^2 + \omega_n^2(1-\xi^2)} \end{aligned} \tag{14}$$

for $0 < \frac{R_a}{2\omega_n L_a} < 1$. This transient equation (14) for the electric charge is obtained after performing several algebraic manipulations so as to find a match in the Laplace transform Tables 2, 3 and 4. The expression $\omega_d = \omega_n\sqrt{1-\xi^2}$ is referred to as the damped natural frequency and nondimensional frequency ratio for the case $0 < \frac{R_a}{2\omega_n L_a} < 1$ is $\frac{\omega_d}{\omega_n} = \sqrt{1-\xi^2}$ where $\xi = \frac{R_a}{2\omega_n L_a}$ and $\omega_n = \sqrt{\frac{\kappa_C}{L_a}}$. Taking the inverse Laplace transform of the transient electric charge $Q_{trs}(s)$ in equation (14) and simplifying, lead to the electric charge as a function of time

$$\begin{aligned} q_{trs}(t) &= ae^{-\xi\omega_n t}\left(\frac{C_1}{\sqrt{C_1^2+C_2^2}}\cos\omega_d t + \frac{C_2}{\sqrt{C_1^2+C_2^2}}\sin\omega_d t\right), \quad \omega_d = \omega_n\sqrt{1-\xi^2} \\ &= ae^{-\xi\omega_n t}(\cos\omega_d t\cos\varphi + \sin\omega_d t\sin\varphi), \quad C_1 = q_0, \quad C_2 = \frac{v_0 + \xi\omega_n q_0}{\omega_d} \\ &= ae^{-\xi\omega_n t}\cos(\omega_d t - \varphi),\ a = \sqrt{C_1^2+C_2^2} \quad \varphi = \tan^{-1}\left(\frac{C_2}{C_1}\right) \end{aligned} \tag{15}$$

where the constants C_1 and C_2 are determined using the initial conditions $q(t_0) = q_0$, and $\dot{q}(t_0) = v_0$. The speed at which the Stirling engine produces the transient current and servomotor torque is determined by the reciprocal of the product of the damping ratio ξ and undamped natural frequency ω_n. Differentiating the expression of the transient electric charge $q_{trs}(t)$ with respect to time gives the transient armature current produced by the Stirling engine. Using the current-torque relationship $\tau_m = k_t i_a(t)$, an explicit expression for the transient torque is also obtained. Selecting and replacing e-waste materials for the Stirling engine component can still produce the voltage required for charging a cell phone as long as the values for the Resistance R_a, inductance L_a and capacitance C are consistent with values in the interval $0 < \frac{R_a}{2\omega_n L_a} < 1$ and undamped natural frequency $\omega_n = \sqrt{\frac{\kappa_C}{L_a}}$ with $\kappa_C = 1/C_a$.

To provide additional guidelines for selecting unused and e-waste component materials to design and build charging systems for Ghana's remote places, we let a to represent

any positive constant voltage that is produced by the Stirling engine. The Laplace transform of the constant voltage $r(t) = a$ is $R(s) = \mathcal{L}(r(t) = \frac{a}{s}$ where the Laplace variable $s \neq 0$. Substituting this expression $R(s) = a/s$ into the function of the electric charge $Q(s)$ in equation (11), we obtain the steady state expression of the electric charge

$$\begin{aligned} Q_{ss}(s) &= a\frac{\omega_n^2}{s(s^2+2\xi\omega_n s+\omega_n^2)} = \frac{ak_1}{s} + \frac{ak_2 s + ak_3}{s^2+2\xi\omega_n s+\omega_n^2} \\ &= a\left(\frac{1}{s} - \frac{s+2\xi\omega_n}{s^2+2\xi\omega_n s+\omega_n^2}\right), \quad k_1 = 1, \quad k_2 = -1, \quad k_3 = -2\xi\omega_n \\ &= a\left(\frac{1}{s} - \frac{s+2\xi\omega_n}{(s+\xi\omega_n)^2+\omega_n^2(1-\xi^2)}\right) \end{aligned} \tag{16}$$

for any positive constant voltage a produced by the Stirling engine and the initial conditions $q_0 = v_0 = 0$.This steady state expression $Q_{ss}(s)$ of the electric charge is due to the constant voltage a produced by the Stirling engine. In this equation (16) the constants k_1 and k_2 are the partial fraction coefficients. The damping ratio ξ lies in the interval $0 < \frac{R_a}{2\omega_n L_a} < 1$ and undamped natural frequency $\omega_n = \sqrt{\frac{\kappa_C}{L_a}}$ with $\kappa_C = 1/C_a$. Taking the inverse Laplace transform of equation (16) and simplifying the algebra, we obtain the electric charge

$$\begin{aligned} q_{ss}(t) &= a\mathcal{L}^{-1}\left(\frac{1}{s} - \frac{s+\xi\omega_n}{(s+\xi\omega_n)^2+\left(\omega_n\sqrt{1-\xi^2}\right)^2} - \right. \\ &\quad \left. \frac{\xi}{\sqrt{1-\xi^2}}\left(\frac{\omega_n\sqrt{1-\xi^2}}{(s+\xi\omega_n)^2+\left(\omega_n\sqrt{1-\xi^2}\right)^2}\right)\right) \\ &= a - ae^{-\xi\omega_n t}\left(\cos\omega_d t + \frac{\xi}{\sqrt{1-\xi^2}}\sin\omega_d t\right) \\ &= a - \frac{ae^{-\xi\omega_n t}}{\sqrt{1-\xi^2}}\left(\sqrt{1-\xi^2}\cos\omega_d t + \xi\sin\omega_d t\right), \quad \omega_d = \omega_n\sqrt{1-\xi^2} \end{aligned} \tag{17}$$

as a function of time. Differentiating $q_{ss}(t)$ with respect to time gives the steady state armature current $i_a(t)$ and substituting the result from the differentiation into the current-torque equation $\tau_m = k_t i_a(t)$ give the steady state expressions for the current and torque, respectively. The heat source, Stirling engine cycles and power transmission from one component to another component in the Stirling engine should be in such a manner that

selected values for the resistance R_a, capacitance C_a and inductance L_a equations must satisfy the expressions in equations (12), (15) and (17) over the interval $0 < \frac{R_a}{2\omega_n L_a} < 1$. These three equations guide the selection of component materials for the Stirling, servomotor, power transmitting mechanism and the cell phone charging system. Experimentally, the team was able to show that the voltage produced by the Stirling engine for charging cell phones in remote places in Ghana was between 4.8 and 5 volts. In the interval (i) $0 < \frac{R_a}{2\omega_n L_a} < 1$, the Stirling engine would generate the voltage for charging cell phones faster than operating the Stirling engine over the intervals (ii) $\frac{R_a}{2\omega_n L_a} = 1$ and (iii) $\frac{R_a}{2\omega_n L_a} > 1$. Both of these two cases have a tendency to be susceptible to greater heat loss than case for $0 < \frac{R_a}{2\omega_n L_a} < 1$. Our testing and experimental observations further showed that the insulation of the heat source can prevent the escape of large amount of heat energy to the surroundings of the Stirling engine. The preferred operating conditions for the Stirling engine to generate sufficient voltage for charging cell phones in Ghana public places are when $0 < \frac{R_a}{2\omega_n L_a} < 1$ and $R_a = 0$ with the undamped natural frequency being $\omega_n = \sqrt{\frac{\kappa_C}{L_a}}$, $\kappa_C = 1/C_a$.

4.2.3 Stirling Engine and Cell Phone Charging

The most common way to charge mobile cell phones is plugging the USB cable of the cell phone into a power supply outlet. Incompatible cell phone chargers or fluctuating current flow through the USB cable could damage the cell phone. Host computer, laptop and other modern electronic devices are alternative ways of charging cell phones through the USB cable. Wireless power transfer, inductive charging coils and electric energy sources enable cell phones to be charged continuously. Worldwide, there are growing expectations to have access to charging systems for cell phones. At conferences, trade shows and mass-gathering public places, people want to get access to cell phone charging systems. The Stirling engine, servomotor and the voltage-current battery constitute our proposed charging system for the people of Ghana. The flywheel, piston-crank shaft, pulleys, belts, bearings, servomotor and other power transmitting mechanisms in the Stirling engine assembly convert the thermomechanical energy into current, voltage and torque. Our test and calculation results showed that the Stirling engine is capable of producing 5 volts. As the intensity of the applied heat source to the Stirling engine

changes, we found the generated voltage to vary between 4.5 volts and 4.8 volts. The adjustments of the pins on the piston-crankshaft, friction between the piston and cylinder and other tolerances supporting the performance of the Stirling engine improved the resulting output voltage.

The performance of the proposed charging system for cell phones is analyzed theoretically by the exponential growth and decay rates of the armature current $i_a(t)$, voltage drops $v_{L_a}(t)$ across the inductance L_a, $v_{R_a}(t)$ across the resistance R_a, and $v_{C_a}(t)$ across the capacitance C_a, and the servomotor torque $\tau_m = k_t i_a(t)$. For the Stirling engine operating conditions satisfying the inequalities (i) $0 < \frac{R_a}{2\omega_n L_a} < 1$, (ii) $\frac{R_a}{2\omega_n L_a} = 1$ and (iii) $\frac{R_a}{2\omega_n L_a} > 1$ with fixed undamped natural frequency $\omega_n = \sqrt{\frac{\kappa_C}{L_a}}$, $L_a \neq 0$, the current $i_a(t)$, voltage drops $v_{L_a}(t)$, $v_{R_a}(t)$, $v_{C_a}(t)$ and torque $\tau_m = k_t i_a(t)$ decay exponentially as the time $t \to \infty$. These three inequalities guide the selection of concrete values for the resistance R_a, inductance L_a, capacitance C_a and amount of the applied heat source on the Stirling engine. The operation of the Stirling engine for values of the servomotor elements in the inequality $0 < \frac{R_a}{2\omega_n L_a} < 1$ will produce sufficient voltage for the charging system. In this case, the performance of both the Stirling engine and servomotor is better than the cases when $\frac{R_a}{2\omega_n L_a} = 1$ and $\frac{R_a}{2\omega_n L_a} > 1$. The Stirling engine produced a voltage for our charging system that is consistent with the same amount of voltage produced by smart devices, host computer, laptop and power supply outlet.

CHAPTER 5. CONCLUSION AND FUTURE RECOMMENDATIONS

Our goal of the project was to design a Stirling engine out of e-waste materials, but due to lack of time, resources, and working on the project remotely we were not able to reach this goal. The official length of time we were intended to work on the project was seven weeks but we quickly realized that this was not enough. Halfway through the seven weeks we had to adjust our approach and modify the objectives but we still hoped to keep the same goal. From week one, we could not begin our first or second objective until we received the Stirling engine in the mail which took more than a week. A large factor that also caused challenges was not being present in Ghana. The five-hour time difference and not having direct access to Agbogbloshie made it difficult to gather all the information we ideally would want. Furthermore, when we met with the ACUC team it was productive and informative but coordinating schedules and finding meeting times was not easy. If we were in person with the ACUC students and e-waste site workers our team believes that project would have been more successful. Although our project was altered throughout the process, we kept many aspects in mind that we provide as recommendations for future work. These recommendations are discussed further in section 5.2.

The following section discusses the collaborative experience with the Ghanaian community and future recommendations to progress the project. Throughout this project, a prominent aspect was our collaboration with the community in Ghana.

Co-design holds emphasis on the relationships between producer, designer, and consumer, the responsibilities that come with each, how they overlap, and how the positions work together. Co-design is important to our project as we want to ensure the sustainability and longevity of the work we accomplish. By using an approach that embodies the ideals of co-design, all the knowledge that our MQP team learns over the term will be simultaneously shared with our partners in Ghana and vice-versa. This means that we are designing collectively and after our MQP has ended, the team in Ghana can continue building the project. Implementing co-design in the project has allowed the ACUC students to continue to work on substituting components and redesigning the Stirling engine out of e-waste parts.

For the future of this project or projects like it the team has suggestions based on the work and observations made throughout the process. One aspect of our testing that has been an obstacle has been how to run the engine without using a direct flame. The engine runs with a flame under the hot cylinder. Heat can be dangerous in any mechanism and too much of it could lead to injuries, explosions, or burns if something goes wrong. With this in mind, the team had to ensure our testing was safe and that we knew how to mitigate an emergency situation. When testing the engine, we wore safety goggles, maintained an appropriate distance from the flame, and always had tongs and water to safely extinguish the fire if anything went wrong. We also made sure to conduct the testing in a laboratory that had the necessary fire safety equipment. The safety precautions we had to take are not sustainable for a household use product. An improvement that may be applied to the engine is an alternative heat source that does not include an open flame. This will improve the safety of the engine as well as the possibility of increasing the efficiency of the engine depending on the source. To improve the design and create a sustainable Stirling engine design, one option is to use solar power instead of fire. Also, the use of renewable energy sources, such as solar power, would minimize the pollutants compared to that of burning isopropyl alcohol.

One goal of the project was to replace the original components on the engine with recycled materials. Reusing and recycling materials is good for the environment as it can create new products without producing additional waste. Without this type of recycling, waste at e-waste sites, like Agbogbloshie, would never get reused and this could lead to an accumulation of waste. This build up would likely take up more space than there is available and it could cause harm to the environment and health of those near it. To continue the design process, more components can be substituted with e-waste. The project focused on structural component replacement but with more time, machining can be implemented on recycled parts to reach the high tolerances we need on the mechanical parts of the engine. The goal here would be to build an engine from scratch using only e-waste materials. This engine could be replicated by others and then sold for profit. Charging a phone is valuable to the Ghanaian community for reasons we have discussed previously. This engine could also be used to charge a battery pack

which would have more versatile capabilities; it could charge other electronics such as computers or headphones. For a future design, the engine can be designed to produce a voltage high enough to sustain charge into a battery pack.

REFERENCES

[1]. Arku, G., Luginaah, I., & Mkandawire, P. (2012). "You either pay more advance rent or you move out": Landlords/ladies' and tenants' dilemmas in the low-income housing market in Accra, Ghana. Urban Studies, 49(14), 3177–3193, from https://doi.org/10.1177/0042098012437748

[2]. Brahambhatt, R. (2021, July 28). The Everlasting, Nearly Emission Free Stirling Engine. Interesting Engineering. Retrieved December 14, 2021, from https://interestingengineering.com/the-everlasting-nearly-emission-free-stirling-engine

[3]. Cassels, S., Jenness, S., Biney, A., Ampofo, W., & Dodoo, N. (2014). Migration, sexual networks, and HIV in Agbogbloshie, Ghana. Demographic Research, 31(28), 821–888. from https://www.demographic-research.org/volumes/vol31/28/31-28.pdf

[4]. Chen, H., Czerniak, S., De La Cruz, E., Frankian, W., Jackson, G., Shieferaw, A., & Stewart, E. (2014, March 28). Design of a Stirling Engine for Electricity Generation. Worcester Polytechnic Institute. Retrieved December 20, 2021, from https://web.wpi.edu/Pubs/E-project/Available/E-project-032814-103716/

[5]. Church, A., Greenbaum, B., Stirling, C., (n.d.) Stirling Engine Fabrication and Design. Worcester Polytechnic Institute. Retrieved March 1, 2022, from https://digital.wpi.edu/show/b8515q00r

[6] Çinar, C., Aksoy, F., & Erol, D., (2012, June 25) The Effect of Displacer Material on the Performance of a Low Temperature Differential Stirling Engine. International Journal of Energy Research, 36(8) 911-917, DOI: https://doi.org/10.1002/er.1861

[7]. Cugurullo, F. (2018, May). The origin of the Smart City Imaginary: From the dawn of modernity to the eclipse of reason.
Research Gate. Retrieved November 14, 2021,
from https://www.researchgate.net/publication/325474312_
The_origin_of_the_Smart_City_imaginary_from_the_dawn_of_modernity
_to_the_eclipse_of_reason.

[8] Daum, K., Stoler, J., & Grant, R. (2017). Toward a more sustainable trajectory for e-waste policy: A review of a decade of E-waste research in Accra, Ghana.
International Journal of Environmental Research and Public Health, 14(2), 135

from https://doi.org/10.3390/ijerph14020135

[9]. Denno, J. (n.d.). Design and analysis of Stirling engines - pcs.cnu.edu. Retrieved December 19, 2021, from https://www.pcs.cnu.edu/~dgore/Capstone/files/DennoJ.pdf

[10]. Dimian, A. C., Bildea, C. S., & Kiss, A. A. (2014). Applied Energy Integration. In Integrated Design and simulation of Chemical Processes 35, 565–598. essay, Elsevier Science.

[11]. Enerdata. (2020) Ghana Energy Information. Enerdata, from https://www.enerdata.net/estore/energy-market/ghana/#:~:text=Total%20Energy%20Consumption,consumption%20was%20485%20kWh%2Fcap.

[12]. Eshun, M. E., & Amoako-Tuffour, J. (2016). A review of the trends in Ghana's power sector. Energy, Sustainability and Society, 6(1). https://doi.org/10.1186/s13705-016-0075-y

[13]. Grant, R. & Oteng-Ababio, M. (2013, May 16) Mapping the Invisible and Real "African" Economy: Urban E-Waste Circuitry. Urban Geology, 33(1). DOI, from https://doi.org/10.2747/0272-3638.33.1.1

[14]. Kuma, P. (2011). Old Fadama-A community under threat. [Web post]. Retrieved from https://philipkumah.wordpress.com/page/3/

[15] Kumi, E. N. (2017) The Electricity Situation in Ghana: Challenges and Opportunities. Washington, DC: Center for Global Development., 2017, from https://www.cgdev.org/sites/default/files/electricity-situation-ghana-challenges-and-opportunities.pdf.

[16]. Kongtragool, B. & Wongwises, S. (2003). A review of solar-powered Stirling engines and low temperature differential Stirling engines. Renewable and Sustainable Energy Reviews, 7(2), 131–154. https://doi.org/10.1016/s1364-0321(02)00053-9

[17]. Larmer, B. (2018, July 5). E-Waste Offers an Economic Opportunity as Well as Toxicity. The New York Times Magazine. Retrieved March 3, 2022 from https://www.nytimes.com/2018/07/05/magazine/e-waste-offers-an-economic-opportunity-as-well-as-toxicity.html#:~:text=In%20the%20United%20States%2C%20which,two%2Dthirds%20of%20heavy%20metals

[18]. Lepawsky, J. & McNabb, C. (2010). Mapping international flows of electronic waste.

The Canadian Geographer / Le Géographe canadien, 54, 177-195. https://doi.org/10.1111/j.1541-0064.2009.00279.x

[19]. Linda Hall Library. (2019, October 25). Scientist of the Day - Robert Stirling. Linda Hall Library. Retrieved March 3, 2022 from https://www.lindahall.org/robert-stirling/

[20]. Lutz, A. E., Larson, R. S., & Keller, J. O. (2002). Thermodynamic comparison of fuel cells to the Carnot cycle. International Journal of Hydrogen Energy, 27(10), 1103–1111. https://doi.org/10.1016/s0360-3199(02)00016-2

[21]. National Society of Professional Engineers (NSPE). (2019). NSPE Code of Ethics for Engineers. National Society of Professional Engineers. Retrieved March 3, 2022 from https://www.nspe.org/resources/ethics/code-ethics

[22]. Nduhuura, P., Garschagen, M., & Zerga, A. (2021, June 20). Impacts of electricity outages in urban households in developing countries: A case of Accra, Ghana. MDPI. Retrieved January 20, 2022, from https://www.mdpi.com/1996-1073/14/12/3676/htm

[23]. Nice, K. (2021, February 9). How Stirling Engines Work. HowStuffWorks. Retrieved December 19, 2021, from https://auto.howstuffworks.com/stirling-engine.htm

[24]. Oppong B. E., Asomani-Boateng, R., & Fricano, R. J. (2020)
Accra's Old Fadama/Agbogbloshie settlement.
To what extent is this slum sustainable?, African Geographical Review, 39(4), 289-307, DOI: https://doi.org/10.1080/19376812.2020.1720753

[25]. Owusu-Adjapong, E. (2018, April 9). Dumsor: Energy Crisis In Ghana. Stanford University,
from https://energyrights.info/sites/default/files/artifacts/media/pdf/dumsor_energy_crisis_in_ghana.pdf

[26]. Panos, E., Densing, M., & Volkart, K. (2016). Access to electricity in the World Energy Council's global energy scenarios: An outlook for developing regions until 2030. Energy Strategy Reviews, 9, 28-49.https://doi.org/10.1016/j.esr.2015.11.003. Retrieved from https://www.sciencedirect.com/science/article/pii/S2211467X15000450

[27]. Quartey, J. D., & Ametorwotia, W. D. (2017). (rep.). Assessing the total economic value of electricity in Ghana: A step toward energizing economic growth. Retrieved from https://www.theigc.org/wp-content/uploads/2018/06/Quartey-Ametorwotia-2017-

Final-report.pdf.

[28]. Ritchie, H. & Roser, M. (2020, November 28). Access to Energy. Our World in Data. Retrieved January 27, 2022, from https://ourworldindata.org/energy-access

[29]. SmartSolar Ghana. (2019, February) Electricity and fuel prices in Ghana. Smart-Solar Ghana. www.smartsolar-ghana2019com/solar-sector-information/electricity-and-fuel-prices-in-ghana/

[30]. Spitzbart, M. (2022, February 10). Environmentally sound disposal and recycling of e-waste in Ghana. Giz. Retrieved February 11, 2022, from https://www.giz.de/en/worldwide/63039.html#:~:text=In%20Ghana%2C%2095%20per%20cent, recycling%20are%20organised%20largely%20informally.&text= The%20most%20important%20location%20is,commonly%20known%20as%20'Agbogbloshie

[31]. National Museums Scotland. (n.d.). Stirling engine model at National Museum of Scotland. Retrieved December 15, 2021, from https://www.nms.ac.uk/explore-our-collections/stories/science-and-technology/stirling-engine/

[32]. Tavakolpour, A. R., Zomorodian, A., & Akbar Golneshan, A. (2008). Simulation, construction and testing of a two-cylinder Solar Stirling engine powered by a flat-plate solar collector without regenerator. Renewabl Energy, 33(1), 77–87. https://doi.org/10.1016/j.renene.2007.03.004

[33]. Urieli, I. (2013, March 30). Stirling engine configurations - updated 3/30/2013. Retrieved December 20, 2021, from https://www.ohio.edu/mechanical/stirling/engines/engines.html

[34]. Valickova, P. & Elms, N. (2021). The costs of providing access to electricity in selected countries in Sub-Saharan Africa and policy implications. Energy Policy, 148 Part A https://doi.org/10.1016/j.enpol.2020.111935

[35]. Walker, G. (1973). THE STIRLING ENGINE. Scientific American, 229(2), 80–87. http://www.jstor.org/stable/24923172

[36]. Woodford, C. (2021, May 28). How do Stirling engines work?. Explain that Stuff. Retrieved December 19, 2021, from https://www.explainthatstuff.com/how-stirling-engines-work.html

[37]. Zohuri, B. (2018). Gas Power and Air Cycles. In Physics of cryogenics: An ultralow temperature phenomenon, 331–385. essay, Elsevier.